FRAGMENTATION IN THE EUROPEAN MONETARY UNION: IS IT REALLY OVER?

Bertrand Candelon, Angelo Luisi , Francesco Roccazzella

REPRINT • 2022 / 01

UCLouvain

LFIN | LIDAM Louvain Institute of Data Analysis and Modeling in economics and statistics

LFIN

Voie du Roman Pays 34, L1.03.01 B-1348 Louvain-la-Neuve

Tel (32 10) 47 43 04

Email: lidam-library@uclouvain.be

https://uclouvain.be/en/research-institutes/lidam/lfin/publications.html

Fragmentation in the European Monetary Union: Is it really over? ⋆

Bertrand Candelon[a], Angelo Luisi[a,1], Francesco Roccazzella[a]

[a] *Université catholique de Louvain, Louvain Finance*

Abstract

Sovereign bond market fragmentation represents one of the major challenges European authorities have had to tackle since the outburst of the euro area debt crisis in 2010. By investigating the inter-country shock transmission through a new methodology that reconciles Factor and Global Vector Autoregressive models, we first show that fragmentation risk well preceded the sovereign debt crisis outburst. Most importantly, by analyzing the recent period, we document a rise in fragmentation risk in the euro area during the COVID pandemic. This rise, connected to the pressure on public debts and deficits due to the pandemic period, questions the European integration process and calls for early measures to avoid a new sovereign debt crisis.

Keywords: Euro Area, Sovereign bond, Fragmentation, COVID.

JEL Classification: F36, F37, G12, H63.

⋆The authors thank the guest editors of the Journal of International Money and Finance, Joshua Aizenman, Yin-Wong Cheung, and Frank Westermann, Paul de Grauwe (discussant), as well as an anonymous referee. The authors are also grateful to Christian Brownlees, Carlo Favero, Daniele Verdini, and the participants at the conference on "Financial Globalization and De-Globalization: Perspectives and Prospects", the UCLouvain CORE Brown Bag, the Insti7 internal seminars, the 7^{th} International Young Finance Scholars Conference, the DEPS reserach seminar at the University of Siena and the 11^{th} RCEA Money-Macro-Finance Conference for useful comments and remarks. This research was conducted as part of the research program entitled "Financial and Extra-Financial Risk Modeling" under the aegis of the Europlace Institute of Finance, a joint initiative with Insti7. The usual disclaimer applies.

Email addresses: `candelonb@gmail.com` (Bertrand Candelon), `angelo.luisi@uclouvain.be` (Angelo Luisi), `francesco.roccazzella@uclouvain.be` (Francesco Roccazzella)

[1]Corresponding author.

1. Introduction

Since the 2010-2012 European Sovereign Debt (ESD) crisis, the evolution of sovereign bonds in the euro area countries has been closely monitored. With the introduction of euro as common currency, long term yields differentials between euro area government bonds started to co-move synchronously at low rates, respecting hence the well-known property of uncovered interest rate parity in fixed exchange rate regimes. The ESD crisis completely changed this setting by leaving place to heterogeneous and unprecedented high levels of divergence among yields. Specifically, high- and low-indebted countries exhibited different patterns. The former experienced increasing yields, the latter decreasing. The fragmentation era began.

De Grauwe and Ji (2012) proved how, during the ESD crisis, only Greece experienced a solvency crisis (i.e., driven by underlying fundamentals), while the other high-indebted countries were instead hit by self-fulfilling liquidity crises (i.e., not based on changes in underlying fundamentals). Furthermore, existing literature outlined how during periods of market distress, euro area sovereign bond market participants tend to (i) dis-invest in bonds of countries exhibiting high debt- and deficit-to-GDP ratios (i.e., temporary shift in preferences, labeled as "contagion", see, for example, Favero and Missale, 2012), and (ii) invest more in safer and more liquid assets (i.e., "flight-to-quality", see, for example, Beber et al., 2009).

It therefore appears evident that, even during such a period of strong yields' co-movement as the pre-ESD crisis, euro area sovereign bond markets were not fully integrated. In fact, bond markets can be considered integrated when bonds are exposed to the same risks (Baele et al., 2004). The observed heterogeneous reaction to the asymmetric Greek solvency crisis proved that fragmentation risk (i.e., countries sovereign bond market heterogeneous exposure to foreign counterparts) preceded the ESD crisis outburst (Candelon and Luisi, 2020).

In this paper, we thus aim at evaluating the presence of a latent fragmentation risk already in the period preceding the ESD crisis outburst. Fragmentation risk is defined in an *out-of-sample* fashion, that is, the risk that a sudden increase in a high-indebted country's yield is associated with (i) an increase in sovereign yields of other high-indebted countries (“contagion”), and (ii) a decrease in financial sounder countries’ yields (“flight-to-quality”).

Moreover, by looking at the current period, one important similarity with the pre-ESD crisis period emerges. Specifically, the global COVID pandemic crisis is putting pressure on sovereign debts and deficits, as the Great Financial Crisis of 2008-2009 also did in the pre-ESD crisis period. Therefore, we also aim at assessing whether a latent risk of sovereign bond market fragmentation is still present nowadays (given the current COVID global crisis).

Tackling fragmentation risk inside the euro area has been one of the major challenges for European authorities. In fact, a fragmented euro area sovereign bond market entails several economic and financial problems. First of all, the risk of a euro area breakup, and the subsequent risk that a euro denominated asset gets devalued or redenominated into a new devalued legacy currency (De Santis, 2019), became sizeable and relevant for sovereign bond markets during the ESD crisis period. Moreover, within a fragmented bond market, both conventional and unconventional monetary policies’ transmission is severely weakened and not effective (Grandi, 2019). Thirdly, euro area sovereign bond market fragmentation also implies several challenges in other markets. As documented by Macchiarelli and Koutroumpis (2016), existing literature proved how fragmentation in the euro area affects corporate bond markets (Zaghini, 2016), retail markets (Al-Eyd and Berkmen, 2013), interbank markets (Gabrieli and Labonne, 2018), and interest rate pass-through (Horvath et al., 2018).

Given the crucial role played by fragmentation risk inside the euro area, this paper aims at (i) modeling inter countries sovereign bond markets’ exposure, (ii) identifying the implications for the stability of the euro area, (iii) assessing European authorities’ responses to both the ESD crisis and the current pandemic.

From a methodological standpoint this paper reconciles Factor Augmented VAR ($FAVAR$) and Global VAR ($GVAR$) literature by employing (static) principal components (PC) as a way to retrieve information regarding cross sectional dependence. Specifically, as in Elhorst et al. (2020), we confirm that in presence of high cross sectional correlation, the first PC captures the common shifts in the level of the entire cross section of sovereign bond spreads.

This factor can be interpreted as the common interdependence trend. Conversely, the second PC can be interpreted as an indicator of the fragility of the euro area sovereign bond market. Specifically, it measures how deep the difference between fragile and financially sounder economies is. We follow the intuition of Bernanke et al. (2005), and retrieve the part of the second PC that is unspanned by the specific local market under analysis (i.e. *foreign* information). We express this component as the weighted average of foreign counterparts in the $GVAR$ fashion (Pesaran et al., 2004), but leaving the sign of the weights unconstrained. Therefore, the analysis of the resulting transmission matrix W provides evidence of the presence of "flight-to-quality" and/or "contagion" effects in the euro area (Candelon and Luisi, 2020).

We apply this framework to the long term yield spreads between the 10 year euro area government bonds and the German safe benchmark over three remarkable periods: the pre-ESD crisis, the post-ESD crisis as well as the recent COVID period. We highlight that signs of "contagion" and "flight-to-quality" effects were indeed already present in the pre-ESD crisis period, pointing out at a latent fragmentation risk between peripheral European countries (Portugal, Italy, Ireland, Greece and Spain) and the core ones (Austria, Belgium, Finland, France, and The Netherlands). Soon after the ESD crisis, the different programs of public bonds purchases enhanced by the European Central Bank successfully reduced the fragmentation risk, leading all European spreads to shrink back slowly but steadily to the pre-ESD crisis levels. The COVID pandemic has pushed again fragmentation risk at the forefront of the results. Despite the implementation of the recovery plan for Europe, "contagion" and "flight-to-quality" risks become evident once again, stressing the revival of fragmentation risk.

The paper is sketched as follows: after a preliminary data analysis in Section 2, the methodology is presented in Section 3. The empirical analysis on the fragmentation risk is performed in Section 4, while Section 5 concludes.

2. Preliminary Data analysis

We start our analysis by examining the dynamics of the long term yield differentials between euro area government bonds. The 10-Year ($10Y$) yields are extracted from Refinitiv Eikon data set and are covering 11 countries (Austria, Belgium, Finland, France, Germany, Greece, Ireland, Italy, The Netherlands, Portugal and Spain) over the period June 2006 - March 2021 and shown in Figure 1. Data are weekly.

What emerges from a first visual inspection is that long term yields differentials between euro area government bonds and the German *safe* benchmark co-move following an unstable pattern over time.

In the following sub-sections, we give a closer look at this dynamics, distinguishing across the pre- (June 2^{nd}, 2006 - March 26^{th}, 2010), during- (April 2^{nd}, 2010 - July 27^{th}, 2012), and post- (August 1^{st}, 2012 -), ESD crisis periods. On the one hand, April 2010 represents the indicative watershed that certifies the beginning of the European sovereign debt crisis. In particular, after the publication of the Greek quarterly national accounts data that signaled a persistent recession for the Hellenic economy starting in 2007, credit rating agencies downgraded the Greek sovereign bonds to the investment grade status in late April 2010, meanwhile the Prime Minister George Papandreou formally requested an international bailout for Greece. On the other hand, on the July 26^{th}, 2012 the President of the European Central Bank (ECB) Mario Draghi pronounced the famous "Whatever it takes" speech, announcing the Outright Monetary Transactions ($OMTs$) to neutralize the risk of a euro breakup.[2]

[2]The verbatim of the speech by Mario Draghi is available at `https://www.ecb.europa.eu/press/key/date/2012/html/sp120726.en.html`

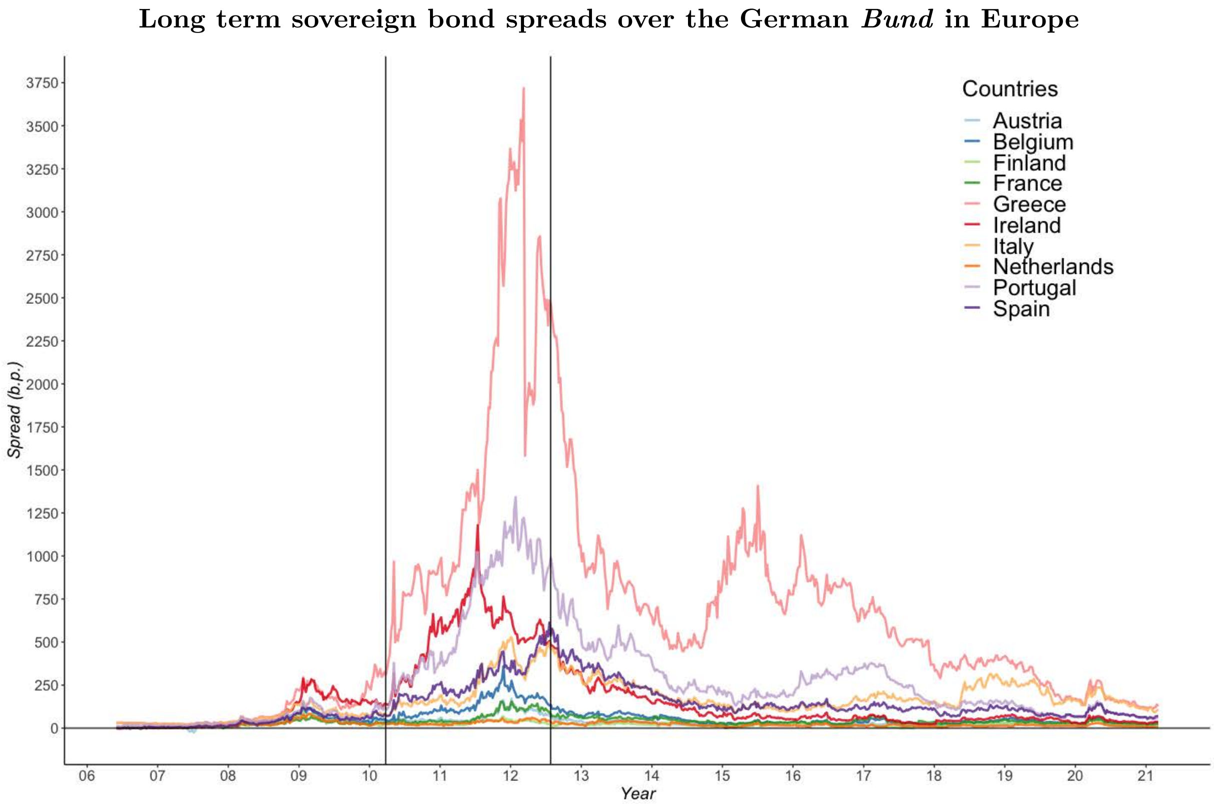

Figure 1: The figure reports the evolution of the government bond yield spread of 10 countries (Austria, Belgium, Finland, France, Greece, Ireland, Italy, the Netherlands, Portugal and Spain) vis á vis of Germany over the period 2006 June - 2021 March. The *EDS* crisis beginning and end dates are indicated with vertical bars.

2.1. Pre-ESD crisis period

The dynamics of the spreads during the pre-*ESD* crisis period can be further decomposed into a convergence period and the subprime loans crisis period. From the introduction of euro as common currency, interest rate differentials co-moved synchronously at a very low level until the burst of the subprime loans crisis. As a reaction to the outburst of the Global Financial Crisis, sovereign spreads substantially increased. The dimension of such an increase firstly proved that investors never regarded different sovereign bonds inside the euro area as perfect substitutes (Favero and Missale, 2012). However, it is worth noticing that, as reported by Copelovitch et al. (2016), during the Great Financial Crisis, European policymakers still regarded the European Monetary Union as an "unquestionable success" and a "rock of macroeconomic stability" helping Europe to weather the Global Financial

Crisis.

2.2. *The ESD crisis period*

The ESD crisis outburst marked the beginning of the euro area fragmentation era. The idea that long term government debt spreads follow a common dynamics in the euro area fades away: the Core (Germany, France, Belgium, Netherlands, and Finland) and Periphery (Greece, Ireland, , Italy, Portugal and Spain) binary classification becomes predominant both in the political and academic debate when analysing the economic and financial turmoil in $2010 - 2012$ (House et al., 2020; Corsetti et al., 2014).

During the fall of 2011, the $10Y$ differentials relative to the German *Bund* reached record heights: Italian $10Y$ sovereign yield spreads rising in a few weeks from 270 basis points in August to over 500 basis points in November. We can draw a similar picture for Ireland, Portugal and Spain. However, such outcomes were only partially connected to underlying fiscal fundamentals (De Grauwe and Ji, 2012), as they mainly reflected self-fulfilling prophecies and the existence of multiple *equilibria* for sovereign bonds' dynamics (Corsetti and Dedola, 2016; Cole and Kehoe, 2000). In the early 2012, the risk of a euro area breakup became so relevant that the Euro redenomination risk, i.e., is the risk that a euro asset is redenominated into a devalued legacy currency, significantly impacted sovereign yield spreads, with Italian and Spanish bonds being most negatively affected (De Santis, 2019).

Following Mario Draghi's, "Whatever it takes" speech, the ECB announced a new set of unconventional measures, the Outright Monetary Transactions ($OMTs$). This programme explicitly aimed at relieving the financial fragmentation in the euro area and at neutralizing redenomination risk. As a fact, by September 2012, Irish, Italian, Portuguese and Spanish differentials relative to the German $10Y$ yield had already decreased by an average of 200 basis points. Through the public purchasing programs (Securities Markets Programme), the very long term refinancing operations ($VLTROs$), and the announcement of the $OMTs$, the ECB mitigated the fears in sovereign bond markets, reinforcing a slow but progressive return of spreads towards normal levels.

2.3. The post-ESD crisis period and the COVID pandemic.

The post-ESD crisis starts in August 2012, spanning the slow but steady return of spreads towards pre-crisis levels. In late 2012, ECB's actions addressed the difficulties in the transmission of the monetary policy measures, the onset of a credit crunch, and the risk of deflation.[3]

As a result of these measures, the consolidated balance sheet of the Eurosystem has more than doubled between 2010 and 2020, starting from $2,002,210$ EUR millions in 2010 and reaching $4,671,425$ EUR millions in 2019.[4] Consequently, given the massive liquidity injections operated by the ECB during the 2012 - 2020 period, the progressive decline of the $10Y$ government bond differentials relative to the German *Bund* should not come as a surprise.

The COVID-19 pandemic outburst caused a sudden increase in sovereign bond spreads around March 2020, when the European spread of the virus caused the enhancement of the first travelling restrictions and lockdown measures across Europe. During this period, the European Commission, the European Parliament and countries of the European Union have jointly been seeking for an agreement to help repairing the economic and social damages

---

[3]More precisely, in July 2013, the ECB began using forward guidance with the goal of strengthening the monetary policy transmission mechanism from short to long term interest rate. In June 2014, the ECB further cut the main marginal lending facility rate to 0.4%, the refinancing operation rate to 0.15% and lowered the deposit facility rate to -0.10%. A series of the targeted longer-term refinancing operations ($TLTROs$) (June 2014, March 2016 and March 2019) have also been used to stimulate bank lending to the real economy. Starting in mid-2014, the ECB also launched the Asset Purchase Programme (APP), conducting net purchases of corporate sector ($CSPP$), public sector ($PSPP$), asset-backed securities ($ABSPP$) and covered bond ($CBPP3$).

[4]The Eurosystem consolidated balance sheet is published together with the Annual Accounts, and is included in the Annual Report of the ECB. The data is available at `https://www.ecb.europa.eu/pub/annual/balance/html/index.en.html`

caused by the Coronavirus pandemic and boost the recovery at the European level. In December 2020, the agreement for a 1.8 trillion EUR recovery plan was reached[5] together with the return of generalized common and declining co-movement in the dynamics of $10Y$ government debt spreads. Among the novelties of the recovery plan, it is worth noticing that it will be issued by the European Union as a whole, and that the associated debt will not be recorded in the countries national accounts. It should result in reducing the risk premium and foster the link among European countries.

3. Empirical analysis

3.1. Modeling sovereign bond spreads in the euro area

GVAR Models (Pesaran et al., 2004) have been employed in the analysis of the interactions among European sovereign bonds spreads as a tool to unveil the tightness of financial interconnectedness and to identify the transmission channels of asymmetric shocks. Favero (2013) showed that the cross correlation among sovereign bond spreads follows an unstable pattern over time, implying that a correct proximity measure should take into account the temporary shifts in investors' preferences when modeling interconnections in the euro area. Moreover, Favero and Missale (2012) showed how a shift in market sentiment following the emergence of a country financial distress can propagate to relatively safer countries. For example, they estimate that a shock in August 2011 could trigger a contagion on the Italian sovereign yield of the size of 200 basis points.

Following Favero and Missale (2012), the local *GVAR* specification in the case of long term sovereign bond spreads over the German *Bunds* $(Y_t^i - Y_t^{DE})$ can be expressed as follows:

$$(Y_t^i - Y_t^{DE}) = \beta_{i0} + \beta_{i1}(Y_{t-1}^i - Y_{t-1}^{DE}) + \beta_{i2}(Y_t^i - Y_t^{DE})^* + \beta_{i3}(Y_{t-1}^i - Y_{t-1}^{DE})^* + u_t^i \quad (1)$$

where $i = 1, \ldots, N$ is the specific country under analysis, β_{i0} the deterministic component,

[5] see https://ec.europa.eu/info/strategy/recovery-plan-europe_en.

β_{i1} the coefficient associated with the country specific lagged variable, and β_{i2} and β_{i3} the coefficients associated with the (contemporaneous and lagged) *Global Spreads*, $(Y_t^i - Y_t^{DE})^*$. *Global Spreads* are computed for each country as the weighted average of foreign counterparts' spreads over the German *Bund*, $\sum_{i \neq j} w_{ij}(Y_t^j - Y_t^{DE})$ for each $i \neq j$.

As recommended by Elhorst et al. (2020), we first perform the *CD*-test (Pesaran, 2021) on the cross section of spreads to prove their strong co-movement along a global trend (see Section 4). Based on this result, we augment the *GVAR* specification in (2) as follows:

$$(Y_t^i - Y_t^{DE}) = \beta_{i0} + \beta_{i1}(Y_{t-1}^i - Y_{t-1}^{DE}) + \beta_{i2}(Y_t^i - Y_t^{DE})^* + \beta_{i3}(Y_{t-1}^i - Y_{t-1}^{DE})^* + \beta_{i4}\hat{F}_{1,t} + u_t^i \quad (2)$$

where $\hat{F}_{1,t}$ is the first Principal Component (PC) extracted from the cross-section of spreads.[6]

The common factor $\hat{F}_{1,t}$ can therefore be interpreted as a long run stable attractor proxying the global interdependence among European countries' sovereign bonds. By augmenting our specification in this way, we make sure that the *star* variables in (2) and the associated coefficients deal with *intra-European* interconnection defined in a *GVAR* fashion.

The choice of the weights employed to build the *Global Spreads* is crucial. The *GVAR* specification demands the weights to summarize the *external* information through a weighted average of foreign counterparts. Existing literature has shown that misspecifying the channel of interconnection results in incorrect inferences (see, for example, Gross, 2019). Candelon and Luisi (2020) show that in the case of euro area sovereign bond spreads, an empirically valid channel of interaction should take into account the asymmetric transmission of shocks among countries that exhibit positive (negative) interconnections.

Therefore, it is natural to start the interconnection analysis from the second factor of the

[6]Observable common variables are often also employed in the literature for this purpose (for example, Favero, 2013, augments the specification with the long term corporate *Baa-Aaa* spread to account for global risk aversion). We refer to the Appendix D for a supplementary analysis of the correlations between the first PC and such observable variables.

cross section of sovereign spreads for several reasons. First, the second Principal Component $\hat{F}_{2,t}$ summarizes the cross sectional information that is linearly independent to the first factor $\hat{F}_{1,t}$, therefore its inclusion in (2) would not be problematic from an econometric perspective. Second, by construction $\hat{F}_{2,t}$ is designed to explain most of the cross sectional variance left unexplained by $\hat{F}_{1,t}$, capturing therefore the interconnection among spreads as we aim to. Third, the loadings of the factors are not constrained to be nonnegative, providing guidance for not only the size, but also the sign of the weight of each local yield contribution to the cross sectional variance explained. Four, it allows us to follow the intuition in Bernanke et al. (2005) and extract from the Principal Component the *foreign* information, as requested by the $GVAR$ framework, where the *Global* variable is a weighted average of foreign counterparts. Finally, the factor summarizing external information as (weakly) exogenous variable can be included in a typical $VARX^*$ fashion (see, for example, Balabanova and Brüggemann, 2017).

For all these reasons, we consider:

$$\hat{F}_{2,it} = \sum_{i \neq j} w_{ij}(Y_t^j - Y_{t-1}^{DE}) + v_{it} \tag{3}$$

for every $i = 1, \ldots, N$ with $\sum_{i \neq j} |w_{ij}| = 1$. $\hat{F}_{2,it}$ is the part of the second Principal Component that is unspanned by the local economy i taken into account (see Appendix A). Usually in the $GVAR$ literature, the weights are constraint to be nonnegative. However, the normalization we propose allows keeping the original properties of the size of the weights (Pesaran et al., 2004), while considering also that sovereign bond spreads' interconnections can be positive and negative. Relaxing the nonnegativity assumption becomes particularly relevant when mechanisms as "contagion" (see Metiu, 2012; Candelon and Tokpavi, 2016) or "flight-to-quality" (Monfort and Renne, 2013) are present. Specifically, during distressed periods, investors prefer safer and more liquid assets. This would result in an outflow of money from the peripheral to the Core countries, causing rising yields for the high indebted euro area members ("contagion") while financial sounder economies could benefit from lower rates ("flight-to-quality"). In our framework, this possibility is not ruled out thanks to the unrestricted sign of the weights.

Once the weights are retrieved by estimating (3) with OLS, we can build the foreign weighted averages and estimate the local $VARX^*$ systems as specified in (2).

Armed with the local coefficients, we can proceed to solving the model in order to retrieve the global reduced form VAR representation (see Appendix B) useful for Generalized Impulse Response analysis.

3.2. A closer look to the first and second PCs of the cross section of euro area spreads.

In our model, $\hat{F}_{1,t}$ refers to the first principal component (PC_1) of the cross section of sovereign bond spreads. As we can see in Figure 2, its loadings are all roughly of the same dimension and sign across countries. Consequently, the first principal component can also be seen as an equally weighted portfolio of all sovereign bonds (up to a scaling factor). To correctly interpret this feature, we refer to the *Level* factor in the term structure literature for a meaningful comparison. Specifically, as in the term structure literature (see, for example, Joslin et al., 2011), the *Level* factor (that exhibits similar weights across maturities) captures shifts in the level of the entire yield curve (across all maturities), in our case, $\hat{F}_{1,t}$ captures shifts in the level of the entire cross section of long term spreads, what we define *interdependence* trend.

Conversely, the loadings of the second principal component (PC_2) are heterogeneous both in sign and dimension. Specifically, across all the time periods considered, they show opposite sign between core and peripheral countries. The second principal component of the term structure of yields (i.e., the *Slope* factor) shows similar characteristics for short and long term maturities. As the *Slope* factor measures how steep the yield curve is, so in our model the second principal component measures how deep the difference between fragile and financially sounder economies is. Therefore, we name this factor the *intra-European fragility* factor.

The relative share of each country in its group is also important for inference. During the pre-ESD crisis period, Italy shows the same sign as low yield countries. However, its relative weight is only of $0.07/1.3 = 5.4\%$ while, for example, Finland represents $0.458/1.3 = 35.2\%$. The relative weights translate into the Italian spread being associated with a peripheral behaviour (i.e., subject to "contagion"). Lastly, the relative share of low and high yield countries in the PC_2 is also easily interpretable. If we look at the post-ESD crisis period, for example, the sum of weights of low yield countries increases to 1.4 while the share of high yield countries decreases to 1.168. This translates into more stable and integrated euro area (no asymmetric exposure to shocks from peripheral countries, even if dimension remains different).[7]

Loading of the first two Principal Components of the cross section of spreads

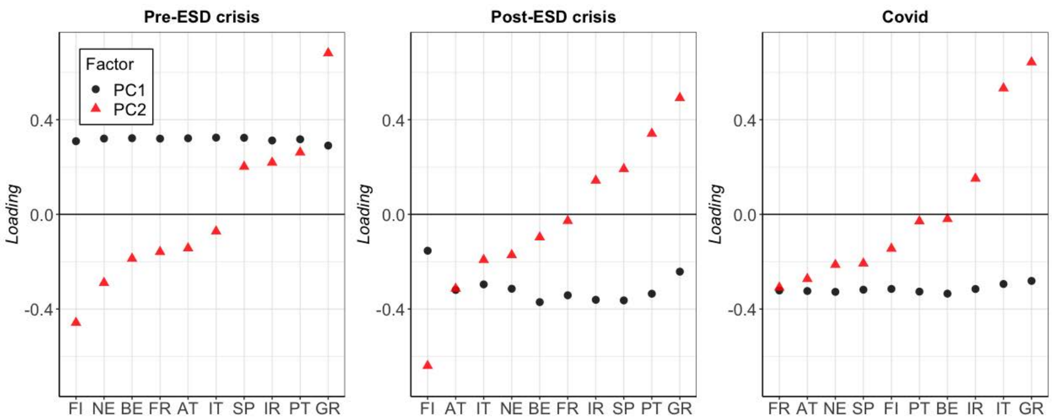

Figure 2: The figure reports the value of the cross sectional loadings of the first two Principal Components of the government bond yield spread of 10 countries (Austria, Belgium, Finland, France, Greece, Ireland, Italy, the Netherlands, Portugal and Spain).

4. Results

4.1. Preliminary results

Following Favero and Missale (2012), and given the data analysis outlined in Section 2, we consider two separate periods: pre-ESD crisis (June 2006 to March 2010) and post-

[7]These facts will be also confirmed by the analysis of the Generalized Impulse Responses in Section 4

ESD crisis (from August 2012 to February 2019). Moreover, the recent COVID period is separately analyzed to further study the last part of the sample, given that, during a period of co-movement at low levels, sovereign bond spreads are exposed to the global pandemic.

The sample split offers several advantages. First of all, by considering homogeneous periods in terms of cross correlation of the spreads, we can assess the changes in interconnectedness in those different phases (Forbes and Rigobon, 2002), while accounting for the observed shifts in market sentiment (Favero, 2013). Furthermore, using a narrative approach, the effect of the unconventional monetary policies in fostering financial integration can be assessed as in Favero and Missale (2016).

The first result reported in Table 1 regards the CD-test to assess the cross sectional dependence of the sovereign spreads under analysis. The CD-test (Pesaran, 2021) is defined as:

$$CD = \sqrt{\frac{2T}{N(N-1)}} \sum_{i=1}^{N-1} \sum_{j=i+1}^{N} \hat{\rho}_{ij}, \tag{4}$$

with $\hat{\rho}_{ij}$ being the sample correlation coefficient between local variables of county i and country j. In Bailey et al. (2016a), we can find the order property of the average correlation coefficient:

$$\bar{\rho}_N = \frac{2}{N(N-1)} \sum_{i=1}^{N-1} \sum_{j=i+1}^{N} \rho_{ij} = O(N^{2\alpha-2}), \tag{5}$$

where $\alpha \in [0, 1]$. As recommended in Elhorst et al. (2020), we first control that the null of weak cross sectional dependence ($\alpha < 0.5$) cannot be rejected in our sub-samples through the CD-test ($\hat{\bar{\rho}}$ and CD-statistic's columns in Table 1). In fact, weak cross sectional dependence cannot be rejected given the high value of $\hat{\bar{\rho}}$.

Secondly, we assess the degree of cross sectional correlation through the two step procedure as in Bailey et al. (2016a).[8] In Table 1 we show that the cross sectional correlation in the sub-samples under analysis is really strong. Specifically, the estimated α is larger than $3/4$, clearly

[8] In the empirical application, we estimate α as in Bailey et al. (2016b)

pointing at the presence of common components at the basis of the behaviour of sovereign spreads. To correctly capture the interconnections among spreads, it is therefore important to *defactorize* the data. Following Vega and Elhorst (2016), we opt for a simultaneous approach as specified in (2).

To further document that *defactorizing* the data is important (and that no interconnection among units is considered at this stage), we show in Table 2 the loadings of the first Principal Component. As expected in such a case, the loadings are evenly distributed among the different sovereign spreads under analysis. Hence, it supports the evidence of a persistent interdependence trend among European sovereign yield spreads (as illustrated in sub-section 3.1).

Table 1: Cross sectional dependence test

	$\hat{\bar{\rho}}$	CD-statistic	$\hat{\alpha}$	$\hat{\sigma}_{\hat{\alpha}}$
Pre-crisis	0.964	91.415	0.7559	0.0213
Post-crisis	0.945	133.355	0.8463	0.0258
COVID-19	0.918	63.409	0.9013	0.0499

Notes: This table reports the estimated average sample correlation between local country i and j, $\hat{\bar{\rho}}$, the cross-sectional test statistics, $CD - statistics$, as well as $\hat{\alpha}$ and its standard error, $\hat{\sigma}_{\hat{\alpha}}$

4.2. Interconnection matrices and their signs

We now proceed to the analysis of the estimated weights. As described in Subsection 3.1, we computed the weights by estimating (3) via OLS. The weights describe the contribution of each $j \neq i$ to the space of the residual unexplained cross sectional variance that is unspanned by country i's sovereign yields, as in Bernanke et al. (2005).

In Tables 3 to 5, we report the weights, row normalized. Therefore, each row i features the tightness and the sign of the interconnection among country i and the foreign counterparts j. By looking at the values, we can easily notice the presence of sign heterogeneity, some weights being positive, while others negative. This feature corresponds to the first signal of the presence of asymmetric interconnection. Specifically, already during the pre-ESD crisis

Table 2: First Principal Component: loadings

	Pre-*ESD*	Post-*ESD*	COVID
Austria	0.321	-0.319	-0.324
Belgium	0.322	-0.371	-0.335
Finland	0.309	-0.154	-0.315
France	0.320	-0.342	-0.322
Ireland	0.312	-0.361	-0.315
Italy	0.324	-0.296	-0.294
The Netherlands	0.320	-0.314	-0.327
Portugal	0.317	-0.335	-0.326
Spain	0.324	-0.363	-0.318
Greece	0.291	-0.242	-0.281
Variance explained	0.922	0.676	0.851

Notes: This table reports the factor loadings of the first static Principal Component over the three periods of investigation and the portion of cross sectional variance explained.

period it was clear the distinction that emerged afterwards in the academic and public debate between Core and peripheral countries. The sovereign yields of Spain, Italy, Portugal, and Greece feature an opposite sign for almost all specifications compared with Austria, Belgium, Finland, France, and The Netherlands. Such a result portraits the "flight-to-quality" phenomenon from peripheral to Core European countries already before the outburst of the *ESD* crisis[9].

During the post-*ESD* crisis period, while Portugal and Greece continue to exhibit the above mentioned features, we can see mixed signs for Ireland and Italy. This result points out at the convergence path started by European countries after the introduction of unconventional monetary policies inside the euro area.

By closely looking at the COVID period of our sample, we can clearly see that the same signs of fragility are back in the sovereign bond market. As a matter of fact, the blocks

[9]This result over the pre-*ESD* crisis sample is coherent with the analysis of Candelon and Luisi (2020) during the period 2001 - 2009. The two periods are indeed similar in terms of cross country sovereign spreads correlations.

of countries exhibiting opposite signs are again Core and Peripherals, with the exception of Belgium, showing some similarities with peripheral countries.

Table 3: Pre-*ESD* crisis period: W matrix

	AU	BE	FN	FR	IR	IT	NL	PT	SP	GR
AU	·	-0.067	-0.258	-0.138	0.035	-0.071	-0.178	0.066	0.089	0.098
BE	-0.037	·	-0.263	-0.158	0.040	-0.088	-0.169	0.060	0.084	0.101
FN	-0.023	-0.083	·	-0.161	0.037	-0.164	-0.233	0.059	0.130	0.110
FR	-0.044	-0.107	-0.275	·	0.036	-0.093	-0.172	0.058	0.106	0.111
IR	-0.056	-0.138	-0.261	-0.089	·	0.002	-0.168	0.085	0.109	0.092
IT	-0.050	-0.086	-0.297	-0.164	0.036	·	-0.132	0.053	0.093	0.089
NL	-0.046	-0.075	-0.298	-0.161	0.039	-0.111	·	0.050	0.104	0.115
PT	-0.086	-0.101	-0.344	-0.071	0.031	0.045	-0.153	·	0.053	0.116
SP	-0.074	-0.078	-0.290	-0.122	0.038	0.006	-0.196	0.096	·	0.099
GR	-0.072	-0.097	-0.205	-0.080	0.022	0.086	-0.224	0.127	0.088	·

Notes: This table reports the weights w_{ij} extracted as indicated in (A.3).

Table 4: Post-*ESD* crisis period: W matrix

	AU	BE	FN	FR	IR	IT	NL	PT	SP	GR
AU	·	-0.091	-0.683	0.052	0.0002	-0.015	-0.088	0.023	0.031	0.017
BE	-0.215	·	-0.509	0.098	-0.035	0.00003	-0.085	0.010	0.033	0.016
FN	-0.227	0.115	·	-0.092	0.048	-0.065	-0.394	0.013	0.023	0.022
FR	-0.211	-0.063	-0.511	·	-0.057	0.014	-0.061	0.019	0.047	0.017
IR	-0.137	-0.227	-0.360	0.200	·	0.017	0.030	0.007	-0.008	0.014
IT	-0.162	-0.026	-0.478	0.108	-0.026	·	-0.137	0.007	0.044	0.012
NL	-0.172	-0.070	-0.557	0.107	-0.025	-0.006	·	0.013	0.035	0.016
PT	-0.176	-0.209	-0.317	0.169	-0.039	0.025	0.033	·	0.018	0.014
SP	-0.158	-0.180	-0.390	0.187	-0.026	0.017	0.021	0.007	·	0.015
GR	-0.124	-0.219	-0.272	0.209	-0.050	0.022	0.049	0.010	0.044	·

Notes: This table reports the weights w_{ij} extracted as indicated in (A.3).

4.3. Impulse response analysis

After the analysis of the transmission matrix W, we further evaluate the properties of the $GVAR$ model by studying the impulse response functions. This analysis provides useful insights when we study a multivariate dynamic systems. In particular, the impulse response

Table 5: COVID period: W matrix

	AU	BE	FN	FR	IR	IT	NL	PT	SP	GR
AU	·	0.026	-0.140	-0.377	0.058	0.063	-0.124	0.040	-0.126	0.047
BE	-0.177	·	-0.107	-0.256	0.068	0.061	-0.210	-0.002	-0.067	0.050
FN	-0.213	0.027	·	-0.317	0.063	0.060	-0.147	0.025	-0.102	0.047
FR	-0.282	0.111	-0.156	·	0.040	0.038	0.007	0.079	-0.232	0.056
IR	-0.165	-0.050	-0.101	-0.174	·	0.066	-0.331	-0.042	-0.013	0.058
IT	-0.192	-0.078	-0.051	0.062	0.068	·	-0.338	-0.093	0.064	0.054
NL	-0.176	0.028	-0.124	-0.344	0.064	0.065	·	0.033	-0.117	0.049
PT	-0.181	-0.002	-0.110	-0.262	0.068	0.061	-0.199	·	-0.067	0.050
SP	-0.143	0.046	-0.142	-0.481	0.042	0.059	-0.015	-0.020	·	0.052
GR	-0.124	-0.090	-0.032	-0.082	0.092	0.069	-0.425	-0.046	0.040	·

Notes: This table reports the weights w_{ij} extracted as indicated in (A.3).

functions map the responses of the system to the effect of shocking one of the variables, at different horizons.

In our GVAR, we have three channels of transmissions of a shock from country i to j: a) via the contemporaneous factor $\hat{F}_{2,t}$, b) its lag $\hat{F}_{2,t-1}$ and c) via the covariance matrix of the errors. Therefore, it is difficult to have a clear identification strategy both when choosing the relevant restrictions in the covariance matrix (Bernanke, 1986; Sims, 1986; Blanchard and Quah, 1989) or when deciding the order of countries and variables in the Orthogonalized Impulse Responses (OIR) (Sims, 1980) set up. The Generalized Impulse Response ($GIRF$) (Pesaran and Shin, 1998; Pesaran et al., 1999) is the standard tool to overcome these limitations in a GVAR framework. $GIRFs$ are invariant to the ordering of the variables and the countries in the $GVAR$, and does not require any restrictions on the covariance matrix of the residuals. In fact, the $GIRF$ considers system shocks and it consists of inducing a one-period shock only on one variable, e.g., the $10Y$ spread of country i, and then, ruling out the historically observed distribution of the errors, predicting the effect of such shock on the system at different horizons.

In the following subsections, we present the generalized impulse response functions in the pre- and post-ESD crisis with a supplementary focus on the COVID pandemic. We build the confidence interval using $10,000$ bootstrap replications (see Appendix C for more details), indicating with a red solid line the median response and with black dotted lines the 16^{th} and 84^{th} confidence bounds.

4.4. Pre-ESD crisis period

Figure 3 reports the generalized impulse responses to a 200 basis points (b.p.) increase of the Spanish $10Y$ differentials. Spain was selected as it is a large peripheral country, which has been quite affected during the ESD crisis period but also by the COVID pandemic.[10]

Our model predicts a fragmentation of the euro area into Core and Periphery even before the beginning of the European sovereign debt crisis (our sub sample precedes the ESD crisis period). Italy, Ireland, Portugal and Greece respond in a similar manner: a 200 b.p. increase of Spanish differentials is associated with increasing differentials in the other peripheral countries.

Beside the sign, the size of such response is also relevant: the estimated increase is well beyond 60 b.p., (150 b.p. for Greece) with the only exception being Portugal. However, the response of Portuguese differential is not statistically significant up to two weeks horizon, but then the predicted increase of the spread becomes significant and particularly persistent.

Conversely, with the exception of Belgium, the 200 b.p. increase of Spanish differentials is associated to a decrease of core economies' spreads: our model predicts the "flight-to-quality" mechanism that will be typically studied in the context of the European Sovereign Debt crisis. A second important aspect that will be a common feature of our results is the humped shape of the $GIRF$. In fact, while the first transmission of the shock occurs at the level of the covariance matrix of the $GVAR$, then subsequent effects and the persistence of the impact are mostly due to the *foreign* factor and its lag. The case of Belgium is exemplary of this: despite

[10] Italy for example has been less affected in term of GDP by the recent pandemic. We refer to the Supplementary Material for the $GIRF$s to a 200 b.p. increase in the spreads of the remaining peripheral countries.

a first significant increase of its differential with respect to Germany (a stylized fact also underlined by Candelon and Luisi, 2020), the $10Y$ spread's response becomes insignificant, dropping in the mild negative territory, aligning Belgium to the other core economies.

Pre-*ESD* crisis

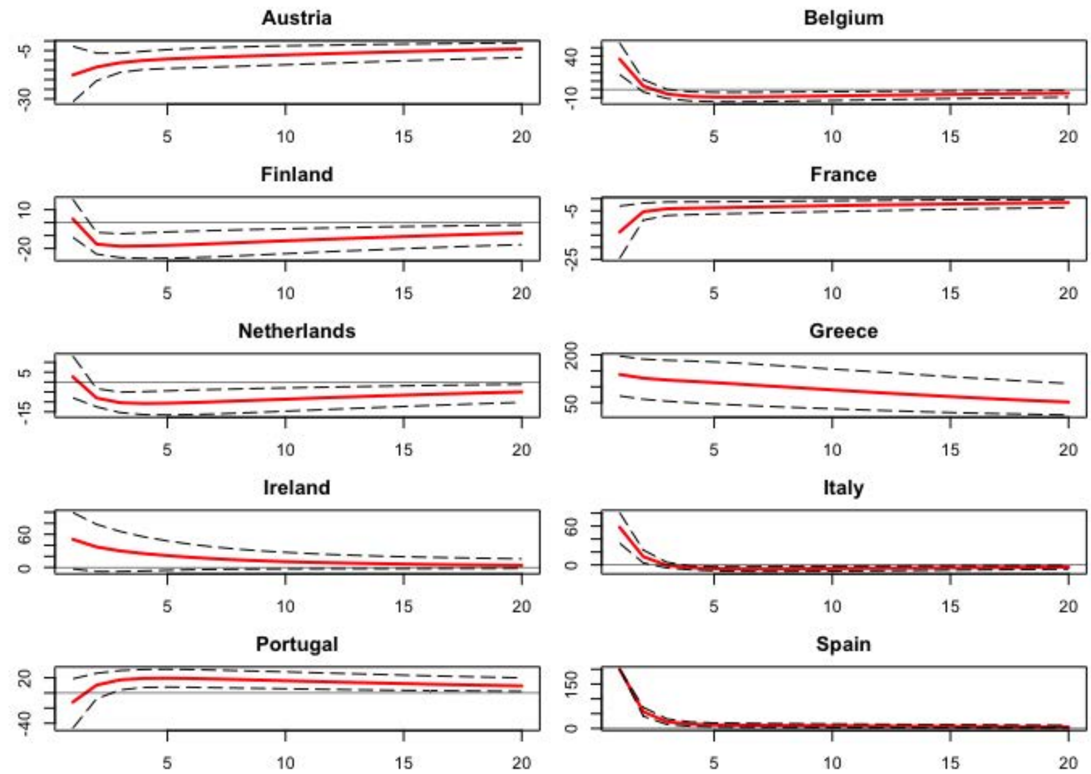

Figure 3: The figure reports the Generalized Impulse Response Functions to a 200 b.p. shock to the $10Y$ Spanish Spread in the pre-crisis period. $[16^{th}, 84^{th}]$ confidence intervals are calculated using $10,000$ bootstrap replications as described in Appendix C.

4.5. Post-*ESD* crisis period

Figure 4 reports the generalized impulse responses to a 200 basis points (b.p.) increase of the Spanish spread. Compared to the pre-*ESD* crisis period, some differences are worth to be underlined. The increase of the Spanish differentials is associated with a generalized statistically significant increase on the spreads of both peripheral and core economies: there are no signals of a "flight-to-quality" mechanism. Nevertheless, there is still a marked difference in the size of the responses: while the response of the core economies is particularly contained in size, the effect of the same increase on the other peripheral country remains important (e.g., over 150 b.p. for Greece) and persistent.

Figure 4 depicts a picture where, despite the perception of the risk of a euro area breakup (no sign heterogeneity in the responses) seems to be vanished, markets still acknowledge the financial fragility of the Periphery relative to the Core (size heterogeneity in the responses).

Post-*ESD* crisis

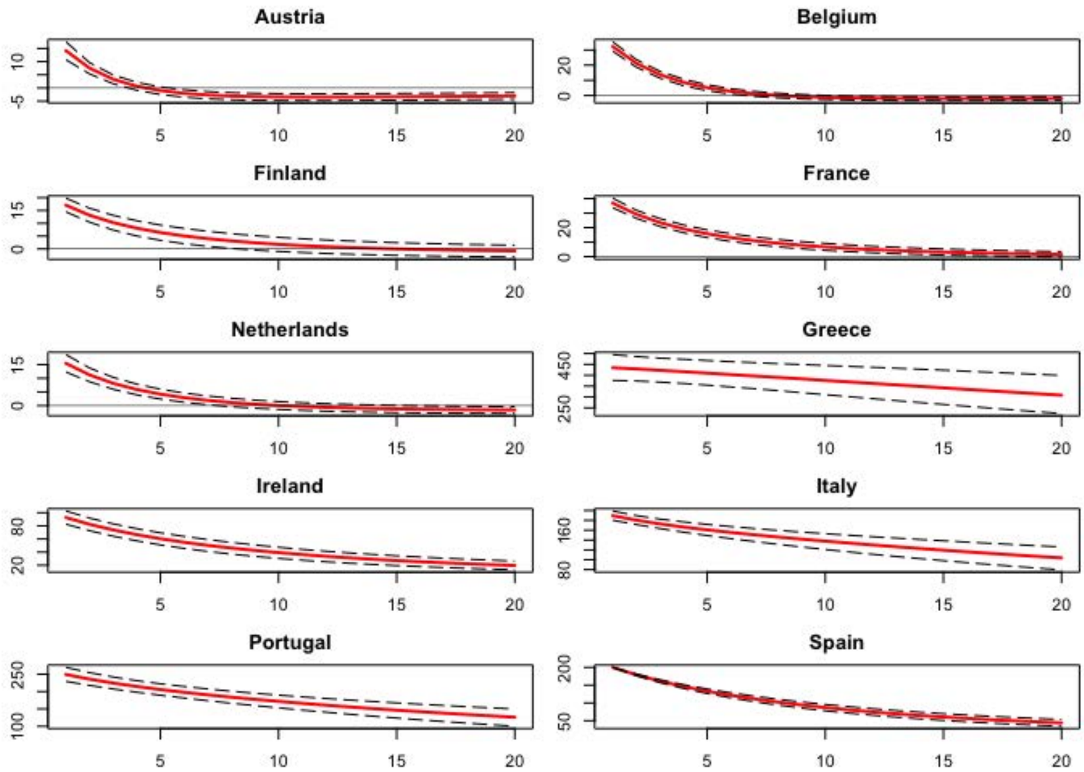

Figure 4: The figure reports the Generalized Impulse Response Functions to a 200 b.p. shock to the 10Y Spanish Spread in the post-crisis period. [16^{th}, 84^{th}] confidence intervals are calculated using 10,000 bootstrap replications as described in Appendix C.

4.6. The COVID pandemic period 2019 *March* - 2021 *March*

As in the previous analyses of the $GIRF$s, we still consider a 200 b.p. increase of the Spanish spreads also in Figure 5.

A question that naturally arises from the analysis of Figure 5 is whether the convergence phase that followed the post-crisis period is over.

In fact, while the size of the responses of the peripheral economies remains somehow unchanged compared to the post-ESD crisis period, Figure 5 depicts a completely different picture compared to Figure 4 with respect the responses of the core economies: the 200 b.p. increase of the 10Y Spanish differentials is now associated with a generalized and statistically significant decrease in the 10Y differentials in core economies. This result highlights the revival of "flight-to-quality" effect, leading to an increase in the *potential* risk of fragmentation of the euro area.

COVID Pandemic

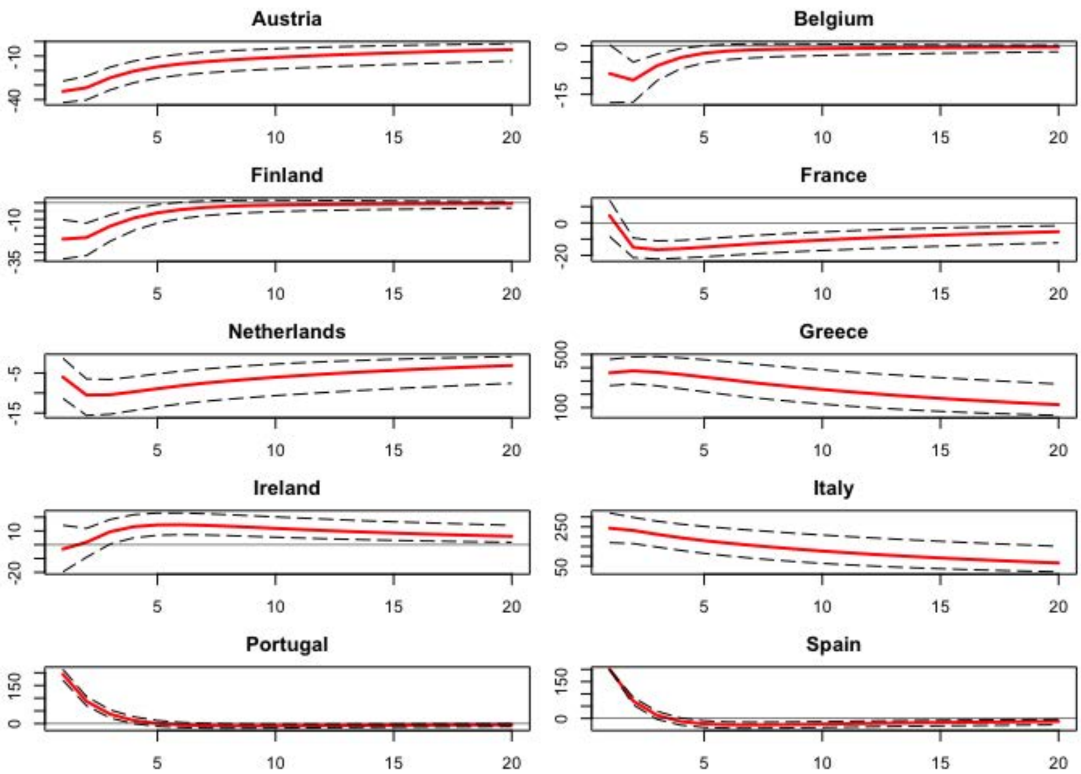

Figure 5: The figure reports the Generalized Impulse Response Functions to a 200 b.p. shock to the 10Y Spanish Spread in the COVID period. [16^{th}, 84^{th}] confidence intervals are calculated using $10,000$ bootstrap replications as described in Appendix C.

4.7. Heatmap: a closer look at the interconnections underlying the $GIRFs$

To summarize the message conveyed by $GIRF$s, we have reported in Figure 6 the heatmap defined by the average correlations of the different $GIRF$ after a 200 basis points (b.p.) shock to the Greek, Irish, Italian, Portuguese and Spanish 10Y differentials.

We hence focus on the signs of the responses to associated to a shock in a peripheral country. To this goal, the heatmap is built on the correlation between the different $GIRF$s obtained after a shock in the spread of a peripheral country for a given forecasting horizon. In our case, we consider a 30 weeks forecasting horizon and the three selected periods: pre-ESD crisis, post-ESD crisis and the COVID pandemic.

Heatmap representation of the Generalized Impulse Response Functions

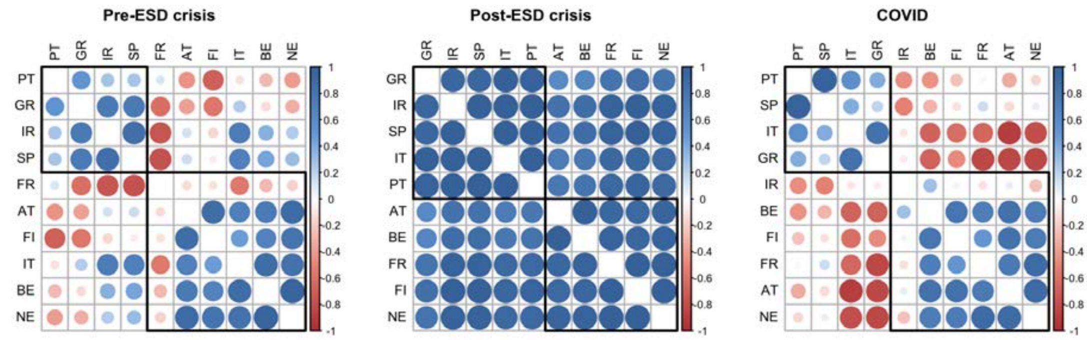

Figure 6: The figure displays the average heatmap representation of the Generalized Impulse Response Functions to a 200 b.p. shock to the 10Y Greek, Spanish, Portuguese and Italian Spreads in the pre-crisis, post crisis and COVID pandemic period with a 30 weeks forecasting horizon. We indicate in blue and red, the positive or negative sign of the correlation between two countries, respectively. The shade of the color and the diameter of the circle represents the intensity of the correlation: the darker (the greater) the circle is, the stronger the correlation is. The rectangles identify the clusters defined by the dissimilarity measure $1 - \rho_{i,j}$, with $\rho_{i,j}$ being the pairwise average correlation coefficient between the $GIRF$ of country i and j to a 200 b.p. shock to Greece, Ireland, Italy, Portugal and Spain.

The fragmentation between Core and Periphery is evident in the pre-ESD crisis period. Ireland, Italy, Greece, Spain and Portugal are strongly and positively correlated together but they are also negatively (or weakly) correlated to the Core European countries. As the sample ends before the ignition of the ESD crisis, this finding confirms the good predictive power of our $GVAR$ model with positive and negative weights in the transmission matrix W. Two countries appear to have a specific role. On the one hand, France is weakly negatively correlated to both peripheral and other Core countries. On the other hand, Italy is the important node that constitutes the junction between both groups: it is positively correlated to Ireland, Greece and Spain but also positively correlated to Austria, Finland, Belgium and Netherlands. This strategic positioning reveals the key role played in the fragmentation risk by this country.

The post-ESD crisis heatmap shows that all the measures enhanced by the ECB have successfully neutralized the devaluation risk and created tighter links between European sovereign bonds. Furthermore, the signs of the interconnections are all strongly positive: this further underlines how, in this period, the euro area sovereign debts behaved as an integrated market. The COVID period heatmap surprisingly looks similar to the pre-ESD crisis one. The degree of similarity amounts to 51.71%, which is well above 0 and quite high when comparing with the post-ESD crisis period (11.70%).[11] Both groups, Core and Periphery, are once again fragmented. Only three slight differences with the pre-ESD crisis can be noticed: first, while Italy joins the group of peripheral countries, Ireland becomes more positively (or weakly) correlated to the core economies, hence leaving the periphery. Second, France is reintegrating its positioning in the European Core. The similarities of the pre-ESD crisis and the COVID periods constitute therefore a clear signal of a resurgence of fragmentation risk in the European Monetary Union.

4.8. Learning from the past: policy implications

The results of the empirical analysis point out at a recent rise of fragmentation risk inside the euro area, defined as heterogeneous exposure of local sovereign bonds to foreign counterparts in the monetary union. Furthermore, the analysis suggests that system shocks generate opposite patterns of responses between core and peripheral countries, as before the pre-ESD crisis outburst.

It is also interesting to notice two characteristics of the first principal component of the cross section of sovereign spreads (proxy for the interdependence trend). While in Table 2 we can see that the cross sectional variance explained by this component raised from 0.67 (post-ESD crisis period) to 0.85 (COVID period), it is worth mentioning that it strongly correlates with the "flight-to-liquidity" measure of Monfort and Renne (2013) during the

[11] We compute the degree of similarity between the heatmaps by the percentage average L1 norm of the difference between the correlation matrices underlying the heatmap representations in the pre-, post-ESD crisis and COVID periods.

recent COVID period (see Appendix D for more details), pointing at a rise of capital flights to safe heavens, coherently with Cheung et al. (2020).

The similarities between the pre-ESD crisis and the COVID periods in terms of fragmentation risk, a resurgence of capital flights to safe heavens, in the context of weakened monetary policy transmission (Corsetti et al., 2020), together with an uncertain global outlook (International Monetary Fund, 2021), demand for adequate policy responses to avoid the triggering of a new sovereign debt crisis. The comparison between the pre-ESD crisis period and the current situation allows to (i) delineate the successful characteristics of the Outright Monetary Transactions (and its eventual criticism), but most importantly (ii) to find correspondence between the $OMTs$ and current measures, allowing for an early evaluation.

In the context of self-fulfilling liquidity crises, the European Central Bank responded successfully with the Outright Monetary Transactions announcement. If we compare the OMTs with the previously implemented Security Market Program, the Outright Monetary Transactions brought the following novelties (i) no *ex ante* limit to the purchases by the European Central Bank, (ii) no seniority status of OMT holdings, and (iii) commitment to fiscal reforms in the context of the European Financial Stability Facility/European Stability Mechanism ($EFSF/ESM$).[12]

However, as stressed in Favero and Missale (2016), the OMTs still exhibit some issues. Specifically, to activate the program, not only *ex ante* eligibility criteria have to be met in terms of sustainable debt, deficit, and sound financial system, but must also *ex post* additional reforms have to be put into actions. If a country under liquidity pressure already satisfies the eligibility criteria, the requirement of additional fiscal adjustments would not only send a wrong signal to the market, but also carry what the authors define as a *stigma* implied by the imposition of fiscal adjustments.

[12]Another difference with the Security Market Program was the focus on maturities between one and three years.

If we now look at the current public rescue package, we can outline some critical features. The first one regards the seniority. One of the reasons the OMTs managed to tackle the panic on the financial markets is that the European Central Bank holdings no longer benefit from seniority status. Multilateral loans in the context of the current public rescue package are expected to have senior stance in case of insolvency. As documented in Steinkamp and Westermann (2014), multilateral loans with senior status do relax the budget constraints of the countries, but do not necessarily have an impact on their effective interest rates.

Secondly, the whole rescue package has a fixed volume while OMTs had no *ex ante* limit to the purchases. Finally, the Next Generation EU Recovery Plan suffers from the same *ex post* conditionality that OMTs holdings had. In fact, partial disbursement of funds will be possible if the intermediate objectives are not achieved. The *ex post* monitoring and the subsequent possibility of only partial disbursement of funds could cause important financial problems in terms of signalling.

Seniority status of the funds, *ex ante* fixed volume, and *ex post* conditionality of funds' disbursements appear to be the bottlenecks of the recent policy responses to ensure that the spreads of less financially sound economies will be more resilient to self fulfilling liquidity crises.

5. Conclusion

This paper sheds new light on the fragmentation risk in the European Monetary Union. A novel methodology reconciling Factor Augmented and Global VAR models allows to disentangle interdependence from "contagion" and "flight-to-quality". It is implemented for yield spreads between 10 year euro area government bonds and the German safe benchmark over three remarkable periods: the pre-ESD crisis, the post-ESD crisis as well as the recent COVID period. We show that signs of "contagion" and "flight-to-quality" effects were already present in the pre-ESD crisis period, pointing out at the latent fragmentation risk between peripheral European countries (Portugal, Italy, Ireland, Greece, and Spain) and the core ones (Austria, Belgium, Finland, France, and The Netherlands). The different measures enhanced by the European Central Banks have limited this risk, leading all European spreads to shrink homogeneously in the the post-ESD crisis period.

The COVID pandemic has reintroduced the fragmentation risk at the forefront of the European sovereign bond market for peripheral countries: similarly to the pre-ESD crisis period, an asymmetric local shock could transmit heterogeneously across countries. This is a new challenge for European policy makers. While ECB's actions to maintain the stability of prices and European Monetary Union under control remain somehow unchanged from the OMTs announcement, the Next Generation EU Recovery Plan, leading to the issuance of European mutualized debt, is the first strong political step towards a deeper fiscal and financial integration in the European Union. The features of such rescue package (i.e., its seniority status, its *ex ante* fixed size, the *ex post* conditionality and public spending monitoring clauses), however, pose also some limits for tackling fragmentation risk in the euro area. If the long term impact of such a package on the interest rates of the peripheral countries turns out not to be effective, fragmentation risk and the heterogeneous transmission of common shocks will remain undisputed obstacles for financial integration in the euro area.

References

Al-Eyd, M. A. J., and Berkmen, P. (2013), *Fragmentation and monetary policy in the euro area*, International Monetary Fund.

Baele, L., Ferrando, A., Hördahl, P., Krylova, E., and Monnet, C. (2004), "Measuring European financial integration," *Oxford Review of Economic Policy*, 20, pp. 509–530.

Bailey, N., Holly, S., and Pesaran, M. H. (2016a), "A two-stage approach to spatio-temporal analysis with strong and weak cross-sectional dependence," *Journal of Applied Econometrics*, 31, pp. 249–280.

Bailey, N., Kapetanios, G., and Pesaran, M. H. (2016b), "Exponent of cross-sectional dependence: Estimation and inference," *Journal of Applied Econometrics*, 31, pp. 929–960.

Balabanova, Z., and Brüggemann, R. (2017), "External information and monetary policy transmission in new EU member states: results from FAVAR models," *Macroeconomic Dynamics*, 21, pp. 311–335.

Beber, A., Brandt, M. W., and Kavajecz, K. A. (2009), "Flight-to-quality or flight-to-liquidity? Evidence from the euro-area bond market," *The Review of Financial Studies*, 22, pp. 925–957.

Bernanke, B. S. (1986), "Alternative explanations of the money-income correlation," *Carnegie-Rochester Conference Series on Public Policy*, 25, pp. 49–99.

Bernanke, B. S., Boivin, J., and Eliasz, P. (2005), "Measuring the effects of monetary policy: a factor-augmented vector autoregressive (FAVAR) approach," *The Quarterly journal of economics*, 120, pp. 387–422.

Blanchard, O. J., and Quah, D. (1989), "The Dynamic Effects of Aggregate Demand and Supply Disturbances," *American Economic Review*, 79, pp. 655–673.

Candelon, B., and Luisi, A. (2020), "Testing for the Validity of W in GVAR models," Tech. rep., Université catholique de Louvain, Louvain Finance (LFIN).

Candelon, B., and Tokpavi, S. (2016), "A non-parametric test for Granger-causality in distribution with application to financial contagion," *Journal of Business & Economic Statistics*, 34, pp. 240–253.

Cheung, Y.-W., Steinkamp, S., and Westermann, F. (2020), "Capital flight to Germany: Two alternative measures," *Journal of International Money and Finance*, 102, p. 102095.

Cole, H. L., and Kehoe, T. J. (2000), "Self-fulfilling debt crises," *The Review of Economic Studies*, 67, pp. 91–116.

Copelovitch, M., Frieden, J., and Walter, S. (2016), "The political economy of the Euro crisis," *Comparative Political Studies*, 49, pp. 811–840.

Corsetti, G., and Dedola, L. (2016), "The Mystery of the Printing Press: Monetary Policy and Self-Fulfilling Debt Crises," *Journal of the European Economic Association*, 14, pp. 1329–1371.

Corsetti, G., Duarte, J. B., and Mann, S. (2020), "The heterogeneous transmission of ecb policies: Lessons for a post-covid europe," *VoxEu*.

Corsetti, G., Kuester, K., Meier, A., and Muller, G. J. (2014), "Sovereign risk and belief-driven fluctuations in the euro area," *Journal of Monetary Economics*, 61, pp. 53–73.

De Grauwe, P., and Ji, Y. (2012), "Mispricing of sovereign risk and macroeconomic stability in the eurozone," *Journal of Common Market Studies*, 50, pp. 866–880.

De Santis, R. (2019), "Redenomination risk," *Journal of Money, Credit and Banking*, 51, pp. 2173–2206.

Elhorst, J. P., Gross, M., and Tereanu, E. (2020), "Cross-sectional dependence and spillovers in space and time: where spatial econometrics and global VAR models meet," *Journal of Economic Surveys*.

Favero, C., and Missale, A. (2012), "Sovereign spreads in the eurozone: which prospects for a Eurobond?" *Economic Policy*, 27, pp. 231–273.

Favero, C. A. (2013), "Modelling and forecasting government bond spreads in the euro area: a GVAR model," *Journal of Econometrics*, 177, pp. 343–356.

Favero, C. A., and Missale, A. (2016), "Contagion in the EMU–the role of Eurobonds with OMTs," *Review of Law & Economics*, 12, pp. 555–584.

Forbes, K. J., and Rigobon, R. (2002), "No contagion, only interdependence: measuring stock market comovements," *The Journal of Finance*, 57, pp. 2223–2261.

Gabrieli, S., and Labonne, C. (2018), "Bad sovereign or bad balance sheets? euro interbank market fragmentation and monetary policy, 2011-2015," .

Grandi, P. (2019), "Sovereign stress and heterogeneous monetary transmission to bank lending in the euro area," *European Economic Review*, 119, pp. 251–273.

Gross, M. (2019), "Estimating GVAR weight matrices," *Spatial Economic Analysis*, 14, pp. 219–240.

Horvath, R., Kotlebova, J., and Siranova, M. (2018), "Interest rate pass-through in the euro area: Financial fragmentation, balance sheet policies and negative rates," *Journal of Financial Stability*, 36, pp. 12–21.

House, C. L., Proebsting, C., and Tesar, L. L. (2020), "Austerity in the aftermath of the great recession," *Journal of Monetary Economics*, 115, pp. 37–63.

International Monetary Fund (2021), "Global financial stability report: Preempting a legacy of vulnerabilities," .

Joslin, S., Singleton, K. J., and Zhu, H. (2011), "A new perspective on Gaussian dynamic term structure models," *The Review of Financial Studies*, 24, pp. 926–970.

Kilian, L. (1998), "Small-sample confidence intervals for impulse response functions," *Review of Economics and Statistics*, 80, pp. 218–230.

Macchiarelli, C., and Koutroumpis, P. (2016), "The current state of financial (dis) integration in the euro area: in-depth analysis," .

Mammen, E. (1993), "Bootstrap and wild bootstrap for high dimensional linear models," *The Annals of Statistics*, pp. 255–285.

Metiu, N. (2012), "Sovereign risk contagion in the eurozone," *Economics Letters*, 117, pp. 35–38.

Miranda-Agrippino, S., and Rey, H. (2020), "U.S. Monetary Policy and the Global Financial Cycle," *The Review of Economic Studies*, 87, pp. 2754–2776.

Monfort, A., and Renne, J.-P. (2013), "Decomposing euro-area sovereign spreads: credit and liquidity risks," *Review of Finance*, 18, pp. 2103–2151.

Pesaran, M., and Shin, Y. (1998), "Generalized impulse response analysis in linear multivariate models," *Economics Letters*, 58, pp. 17–29.

Pesaran, M. H. (2021), "General diagnostic tests for cross-sectional dependence in panels," *Empirical Economics*, 60, pp. 13–50.

Pesaran, M. H., Schuermann, T., and Weiner, S. M. (2004), "Modeling regional interdependencies using a global error-correcting macroeconometric model," *Journal of Business & Economic Statistics*, 22, pp. 129–162.

Pesaran, M. H., Shin, Y., and Smith, R. P. (1999), "Pooled mean group estimation of dynamic heterogeneous panels," *Journal of the American Statistical Association*, 94, pp. 621–634.

Sims, C. A. (1980), "Macroeconomics and reality," *Econometrica*, 48, pp. 1–48.

——— (1986), "Are forecasting models usable for policy analysis?" *Quarterly Review*, 10, pp. 2–16.

Steinkamp, S., and Westermann, F. (2014), "The role of creditor seniority in Europe's sovereign debt crisis," *Economic Policy*, 29, pp. 495–552.

Vega, S. H., and Elhorst, J. P. (2016), "A regional unemployment model simultaneously accounting for serial dynamics, spatial dependence and common factors," *Regional Science and Urban Economics*, 60, pp. 85–95.

Zaghini, A. (2016), "Fragmentation and heterogeneity in the euro-area corporate bond market: Back to normal?" *Journal of Financial Stability*, 23, pp. 51–61.

Appendix A. How to retrieve the country specific weights

Following the intuition of Bernanke et al. (2005), we employ the following methodology to extract foreign information from the second Principal Component of the cross section of spreads:

1. Extract the second Principal Component ($\hat{F}_{2,t}$) of the cross section of spreads.
2. Regress the second Principal Component on the specific local spread I under analysis.

$$\hat{F}_{2,t} = \gamma_i(Y_t^i - Y_t^{DE}) + \nu_{it}. \tag{A.1}$$

3. Clean the second Principal Component from the information spanned by country i

$$\hat{F}_{2i,t} = \hat{F}_{2t} - [\hat{\gamma}_i(Y_t^i - Y_t^{DE})]. \tag{A.2}$$

4. Obtain the external information as average of foreign spreads.
5. Repeat 2 - 5 for each i.

$$\hat{F}_{2,it} = \sum_{i \neq j} w_{ij}(Y_t^j - Y_{t-1}^{DE}) + v_{it}. \tag{A.3}$$

6. Estimate equation A.3 and retrieve the weights.

Appendix B. Solution to GVAR Models

The $GVAR$ framework employs country specific ones built as weighted averages of foreign counterparts, where the weights capture the tightness of the interconnection between country i and country j as follows:

$$x_{it}^* = \sum_{j=0}^{N} w_{ij} x_{jt}, \quad w_{ii} = 0, \quad \sum_{j=0}^{N} w_{ij} = 1 \tag{B.1}$$

resulting in the local *VARX** model.

$$\Phi_i(L, p_i)x_{it} = a_{i0} + a_{i1}t + \Upsilon_i(L, q_i)d_t + \Lambda_i(L, q_i)x^*_{it} + \nu_{it}, \tag{B.2}$$

where p_i and q_i are the maximum lag considered for the local and foreign variables, respectively. The different coefficients are treated as unrestricted for estimation purposes.

Once local parameters in (B.2) are estimated, we can simultaneously solve the model to obtain the *Global VAR* representation of the world. We now summarize the procedure as in Pesaran et al. (2004).

Define the $(k_i + k^*_i) \times 1$ vector:

$$z_{i,t} = \begin{pmatrix} x_{i,t} \\ x^*_{i,t} \end{pmatrix} \tag{B.3}$$

and rewrite (B.2) as:

$$A_i z_{i,t} = B_i z_{i,t-1} + \epsilon_{it} \tag{B.4}$$

with $A_i = (I_{k_i},\ -\Lambda_{i0})$ and $B_i = (\Phi_i,\ \Lambda_{i1})$. For ease of explanation, we here abstract, without loss of generality, from including the deterministic component, the time trend, and additional lags.

If we collect all the local variables in $x_t = (x'_{0t}, x'_{1t}, \ldots, x'_{Nt})'$ for $i = 1, \ldots, N$ with $k = \sum_1^N k_i$, we can rewrite:

$$z_{i,t} = W_i x_t. \tag{B.5}$$

By substituting (B.5) into (B.4), we obtain:

$$A_i W_i x_t = B_i W_i x_{t-1} + \epsilon_{it}, \tag{B.6}$$

Stacking all the equations together:

$$Gx_t = Hx_{t-1} + \epsilon_t, \tag{B.7}$$

As in Candelon and Luisi (2020), by defining the interaction matrix $\tilde{W}$ as:

$$x_t^* = \tilde{W}x_t. \tag{B.8}$$

We can express the matrices G and H as:

$$G = [I_k - \tilde{\Lambda}_0\tilde{W}] \tag{B.9}$$

$$H = [\tilde{\Phi} + \tilde{\Lambda}_1\tilde{W}] \tag{B.10}$$

Lastly, we can retrieve the $GVAR$ solution as:

$$x_t = G^{-1}Hx_{t-1} + G^{-1}\epsilon_t. \tag{B.11}$$

Therefore, the $GVAR$ solution is the reduced form VAR representation of the world. This representation is particularly useful for forecasting, scenario analysis and Generalized Impulse Response function.

Appendix C. Bootstrap procedure for the GIRF confidence bounds

The advantages of the bootstrapping procedure when computing confidence intervals for impulse responses in the VAR framework are described in Kilian (1998). In our framework, to take into account also unknown forms of heteroskedasticity, we proposed the wild bootstrapped procedure as in Mammen (1993). Specifically,

1. Estimate the local $VARX^*$ parameters in eq. (2) (after retrieving the weights as

outlined in Appendix B), and the corresponding residuals u_t^i for each $i = 1, \dots, N$.

2. Following the procedure outlined in Section Appendix B, simultaneously solve the model to get the global VAR representation as of (B.11)

$$(Y_t - Y_t^{DE}) = G^{-1} H (Y_{t-1} - Y_{t-1}^{DE}) + G^{-1} u_t \tag{C.1}$$

with

$$(Y_t - Y_t^{DE}) = ((Y_t^1 - Y_t^{DE})', (Y_t^2 - Y_t^{DE})', \dots, (Y_t^N - Y_t^{DE})')', \tag{C.2}$$

$$G = [I_N - (diag(\beta_{12}, \beta_{22}, \dots, \beta_{N2})\tilde{W})], \tag{C.3}$$

$$H = [(diag(\beta_{11}, \beta_{21}, \dots, \beta_{N1}) + (diag(\beta_{13}, \beta_{23}, \dots, \beta_{N3})\tilde{W})], \tag{C.4}$$

$$u_t = (u_t^{1\prime}, u_t^{2\prime}, \dots, u_t^{N\prime})' \tag{C.5}$$

3. Draw with replacement the sequence of errors $\{\tilde{u}_t\}_{t=2}^T = \{\tilde{u}_t^1, \dots, \tilde{u}_t^N\}_{t=2}^T = \{k_t \hat{u}_t^1, \dots, k_t \hat{u}_t^N\}_{t=2}^T$ with

$$k_t = \begin{cases} \frac{1+\sqrt{5}}{2}, & \text{with probability } p = \frac{\sqrt{5}-1}{2\sqrt{5}} \\ \frac{1-\sqrt{5}}{2}, & \text{with probability } 1-p. \end{cases}$$

as in Mammen (1993), $\tilde{u}_t$ are the stacked estimated local errors.

4. Generate the bootstrapped data sample according to equation C.1. The initial values are the actual ones, and u_t is replaced by the bootstrapped $\tilde{u}_t$.

5. Estimate the local $VARX^*$ on the bootstrapped data sample and compute the corresponding Generalized Impulse Responses.

6. Repeat 3 - 5 a large number of times (in our example, we repeat the procedure 10,000 times), and then extract the quantiles needed.

Appendix D. Analysis of the interdependence factor

In this section, we investigate how the first PC, the interdependece factor, is associated to the observed variables that are often employed in the literature for the same purpose. Specifically, we consider the long term corporate *Baa-Aaa* spread to account for global risk aversion (Favero, 2013); the 10Y US treasury yield (Miranda-Agrippino and Rey, 2020); oil prices; equity market volatility; devaluation risk (De Santis, 2019) and the flight-to-liquidity factor (Monfort and Renne, 2013).

Table D.6 shows the pairwise correlation between the first PC and the aforementioned observable global factors in the Pre-ESD, Post-ESD and COVID periods. While the negative sign of the correlations in the Post-ESD and COVID period reflects the negative loadings of the first PC in the respective samples, our unobserved global trend is strongly correlated with the average devaluation risk in the euro area. We can also notice that while oil prices are correlated with the global trend mainly in the Post-ESD period, flight-to-liquidity (KfW-Bund) and global risk aversion (Baa-Aaa) are strongly correlated with the first PC in the Pre-ESD and COVID period. Therefore, despite the intensity of correlations varies across the sub-samples we considered, the first PC is related with factors that capture devaluation risk, flight-to-liquidity mechanisms and shifts global risk aversion, further supporting the use of the first PC as global trend.

Table D.6: First Principal Component: bilateral correlation with proxies of global factors.

Instrument	Pre-*ESD*	Post-*ESD*	COVID	Risk
VSTOXX	0.02	-0.08	-0.36	Equity Volatility
QUANTO CDS	0.63	-0.90	-0.71	Devaluation
KfW-Bund	0.79	0.13	-0.92	Flight-to-Liquidity
OIL-Brent	-0.31	-0.64	0.24	Inflation
OIL-WTI	-0.29	-0.70	0.32	Inflation
Baa-Aaa	0.81	-0.11	-0.67	Global Risk Aversion
US 10Y	-0.89	0.16	-0.19	Global Financial Cycle

Notes: This table reports the bilateral correlation between the first *PC* and the observable global factors in the Pre-*ESD*, Post-*ESD* and COVID periods. The VSTOXX Indices are based on EURO STOXX 50 realtime options prices and are designed to reflect the market expectations of near-term up to long-term volatility by measuring the square root of the implied variance across all options of a given time to expiration. QUANTO CDS is defined as the average of German, Italian, French and Spanish spreads between 5Y QUANTO CDS denominated in EUR and USD as in Favero and Missale (2016). As in Monfort and Renne (2013),we consider the average spreads across maturities between bonds issued by a German agency (KfW) and their sovereign counterparts to identify liquidity-pricing effects. Indeed, KfW's liabilities are guaranteed by the German government, and therefore, these spreads are essentially liquidity-driven and can be used as a proxy of the flight-to-liquidity mechanism. OIL-Brent (DCOILBRENTEU) and Oil-WTI (DCOILWTICO) are Crude Oil Prices measured in US dollar per barrel.

Supplementary Material

Pre-*ESD* crisis

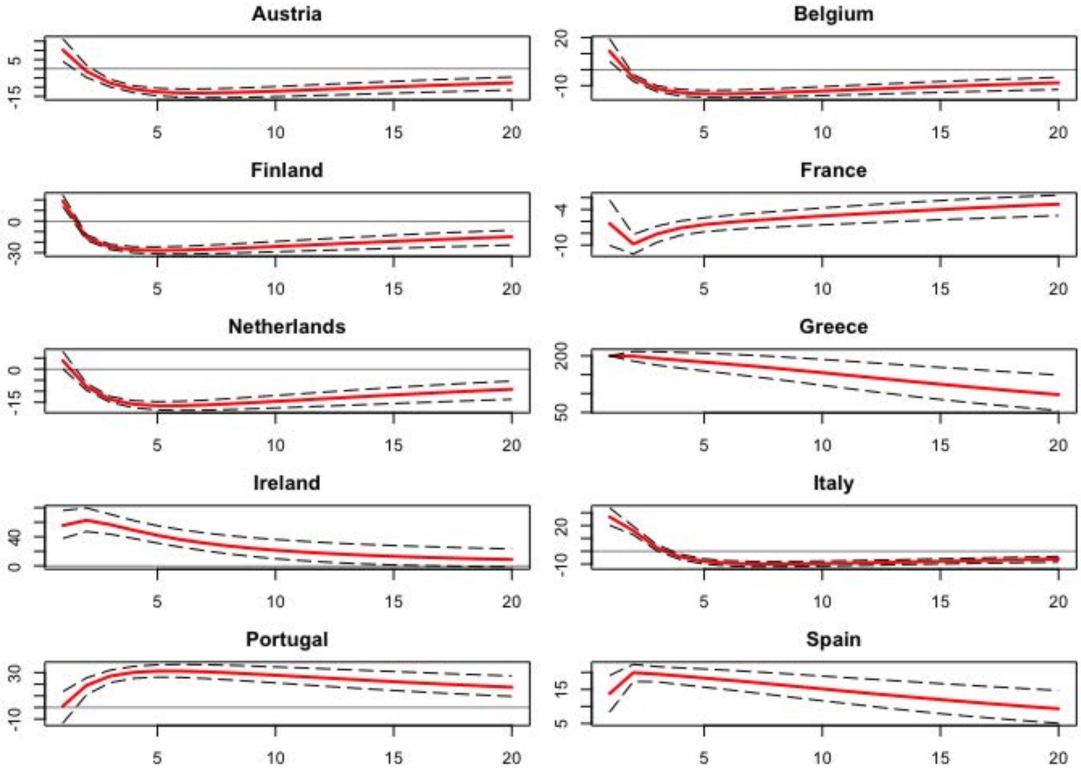

Figure D.7: The figure reports the Generalized Impulse Response Functions to a 200 b.p. shock to the 10Y Greek Spread in the pre-crisis period. [16^{th}, 84^{th}] confidence intervals are calculated using $10,000$ bootstrap replications as in Appendix C.

Post-*ESD* crisis

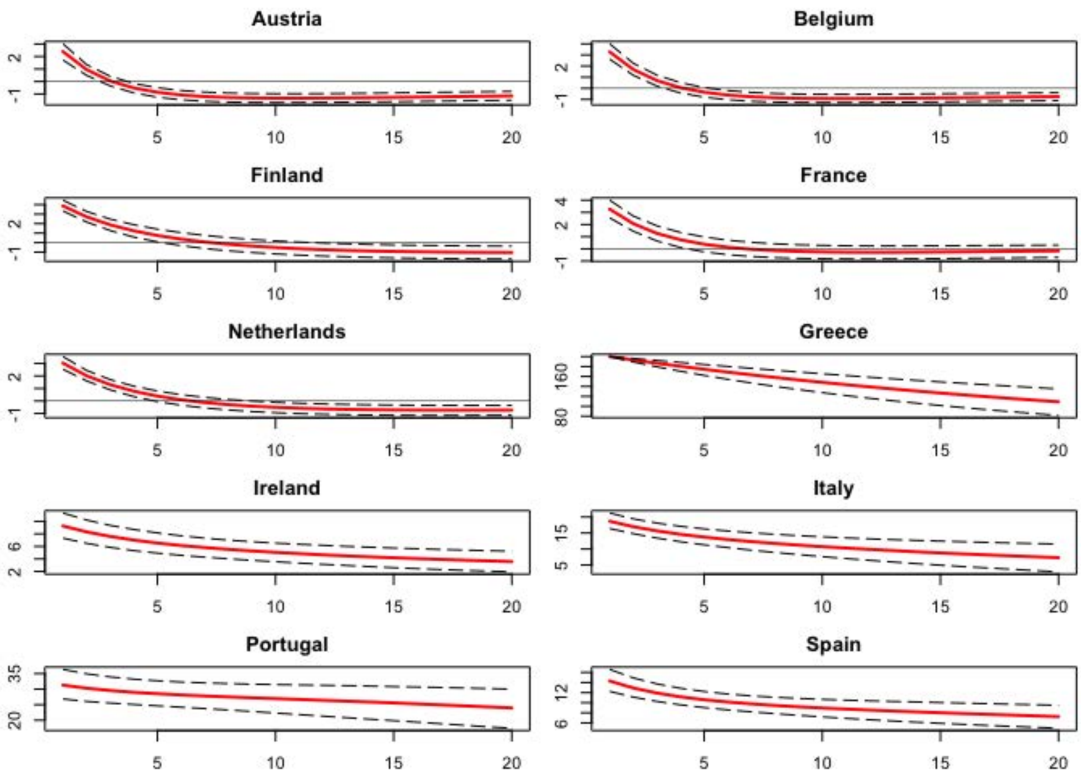

Figure D.8: The figure reports the Generalized Impulse Response Functions to a 200 b.p. shock to the 10Y Greek Spread in the post-crisis period. [16^{th}, 84^{th}] confidence intervals are calculated using $10,000$ bootstrap replications as in Appendix C.

COVID pandemic

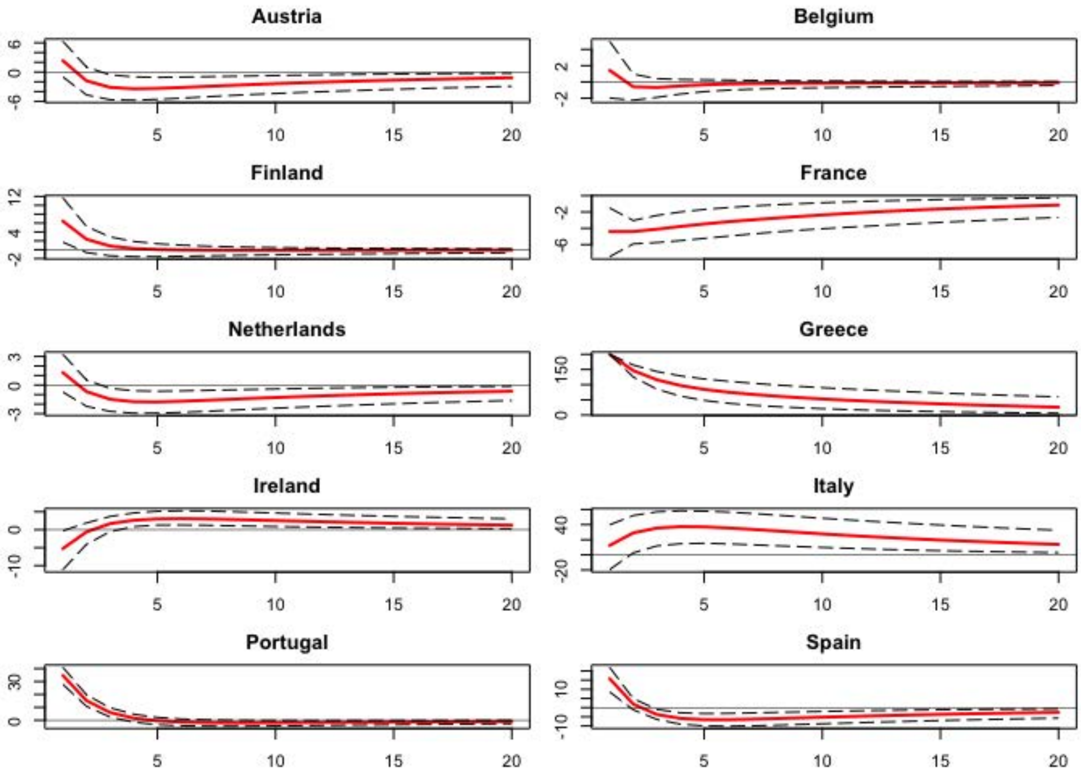

Figure D.9: The figure reports the Generalized Impulse Response Functions to a 200 b.p. shock to the 10Y Greek Spread in the COVID pandemic period. [16^{th}, 84^{th}] confidence intervals are calculated using $10,000$ bootstrap replications as in Appendix C.

Pre-*ESD* crisis

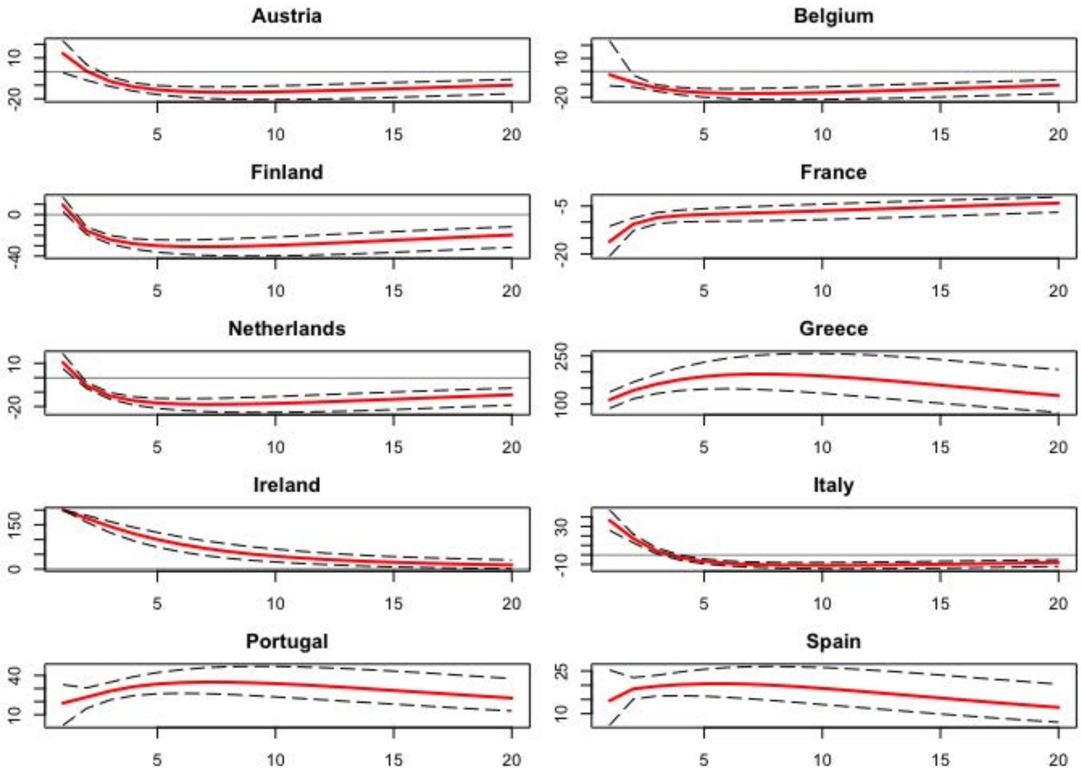

Figure D.10: The figure reports the Generalized Impulse Response Functions to a 200 b.p. shock to the 10Y Irish Spread in the pre-crisis period. [16^{th}, 84^{th}] confidence intervals are calculated using 10,000 bootstrap replications as in Appendix C.

Post-*ESD* crisis

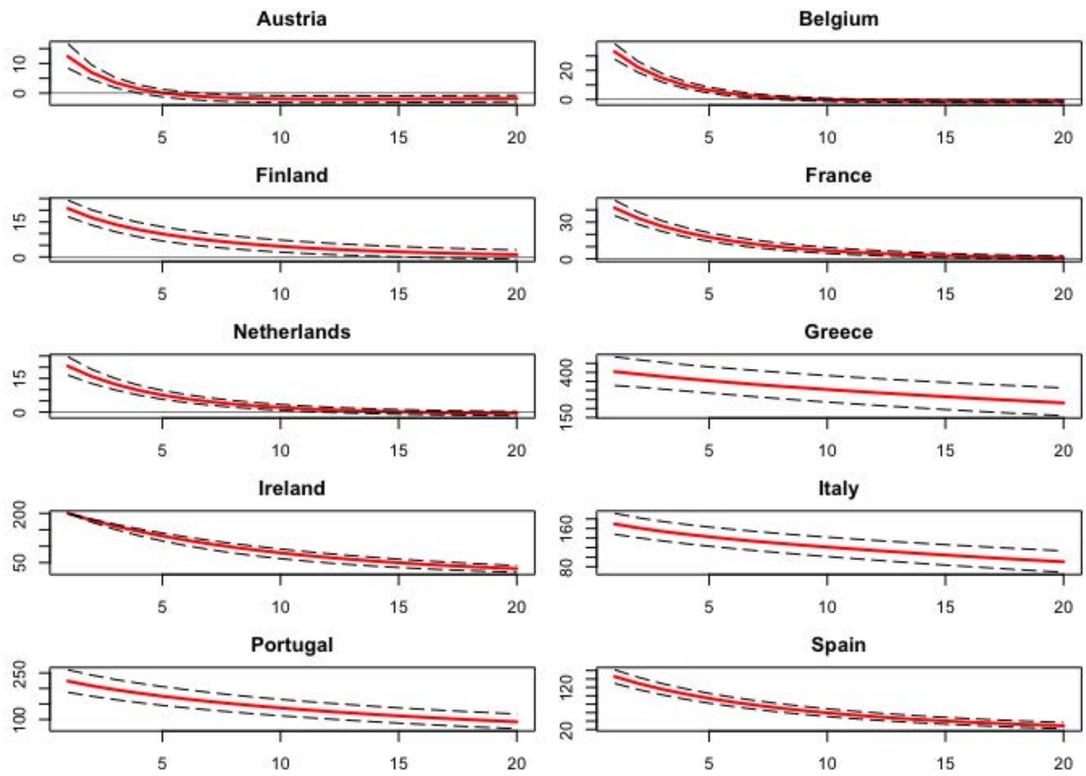

Figure D.11: The figure reports the Generalized Impulse Response Functions to a 200 b.p. shock to the 10Y Irish Spread in the post-crisis period. [16^{th}, 84^{th}] confidence intervals are calculated using $10,000$ bootstrap replications as in Appendix C.

COVID pandemic

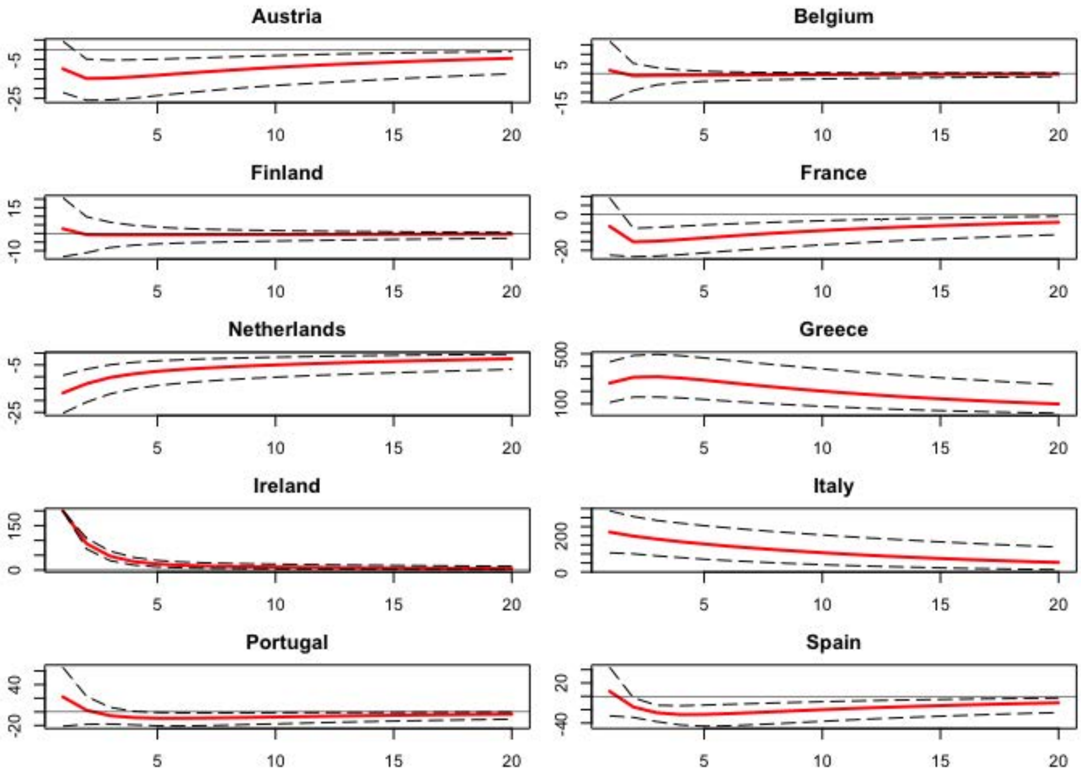

Figure D.12: The figure reports the Generalized Impulse Response Functions to a 200 b.p. shock to the 10Y Irish Spread in the COVID pandemic period. [16^{th}, 84^{th}] confidence intervals are calculated using 10,000 bootstrap replications as in Appendix C.

Pre-*ESD* crisis

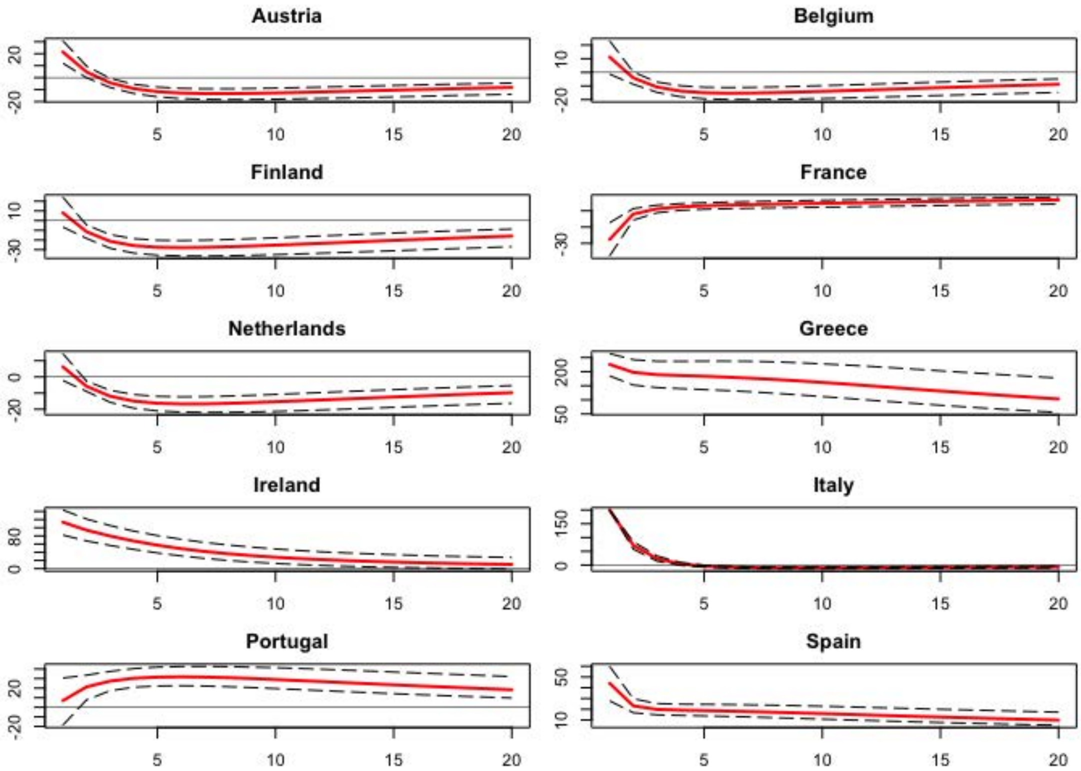

Figure D.13: The figure reports the Generalized Impulse Response Functions to a 200 b.p. shock to the 10Y Italian Spread in the pre-crisis period. [16^{th}, 84^{th}] confidence intervals are calculated using $10,000$ bootstrap replications as in Appendix C.

Post-*ESD* crisis

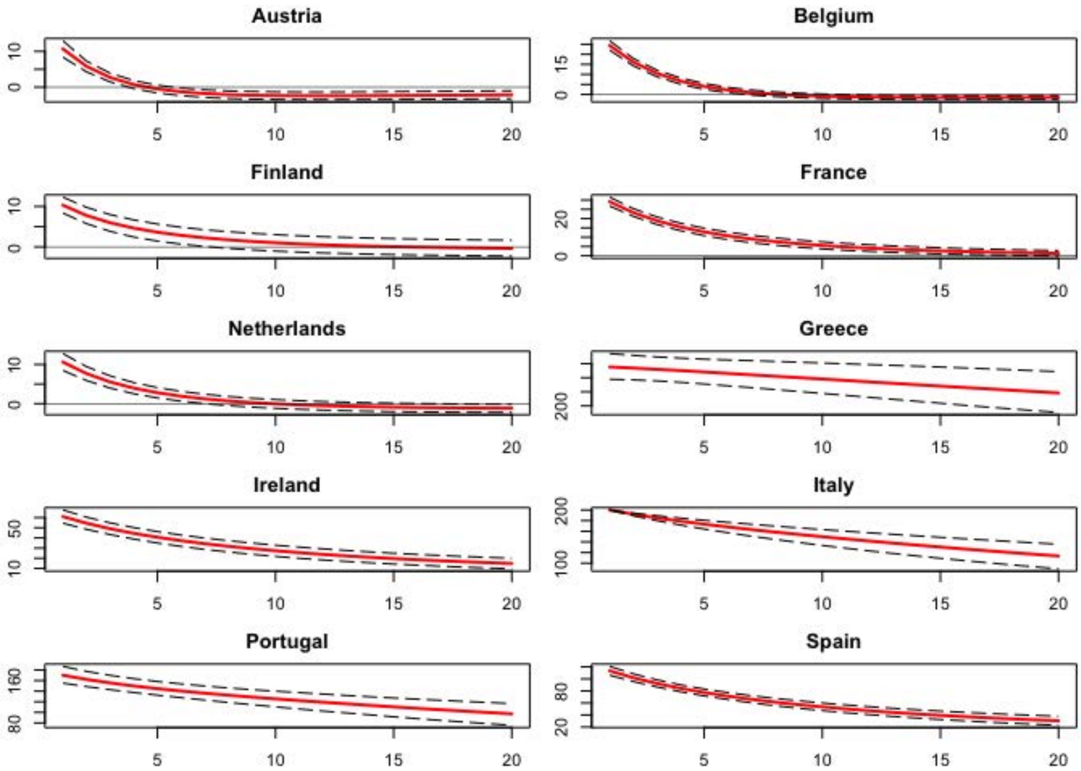

Figure D.14: The figure reports the Generalized Impulse Response Functions to a 200 b.p. shock to the 10Y Italian Spread in the post-crisis period. [16^{th}, 84^{th}] confidence intervals are calculated using 10,000 bootstrap replications as in Appendix C.

COVID pandemic

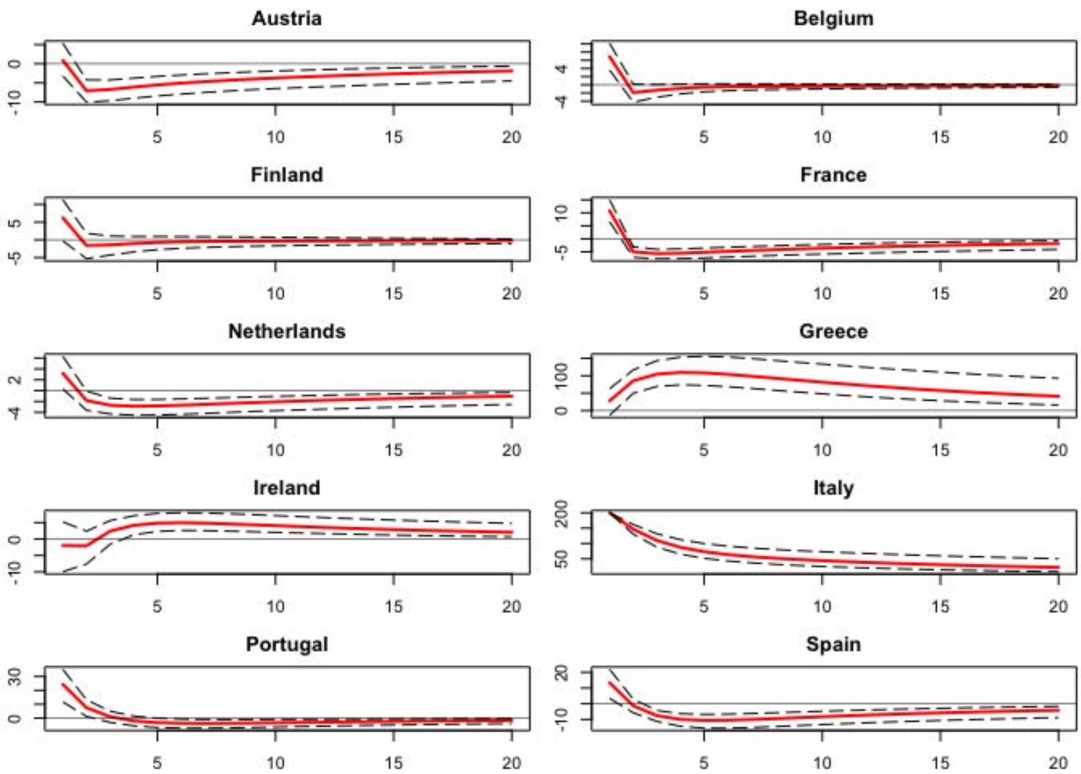

Figure D.15: The figure reports the Generalized Impulse Response Functions to a 200 b.p. shock to the 10Y Italian Spread in the COVID pandemic period. $[16^{th}, 84^{th}]$ confidence intervals are calculated using $10,000$ bootstrap replications as in Appendix C.

Pre-*ESD* crisis

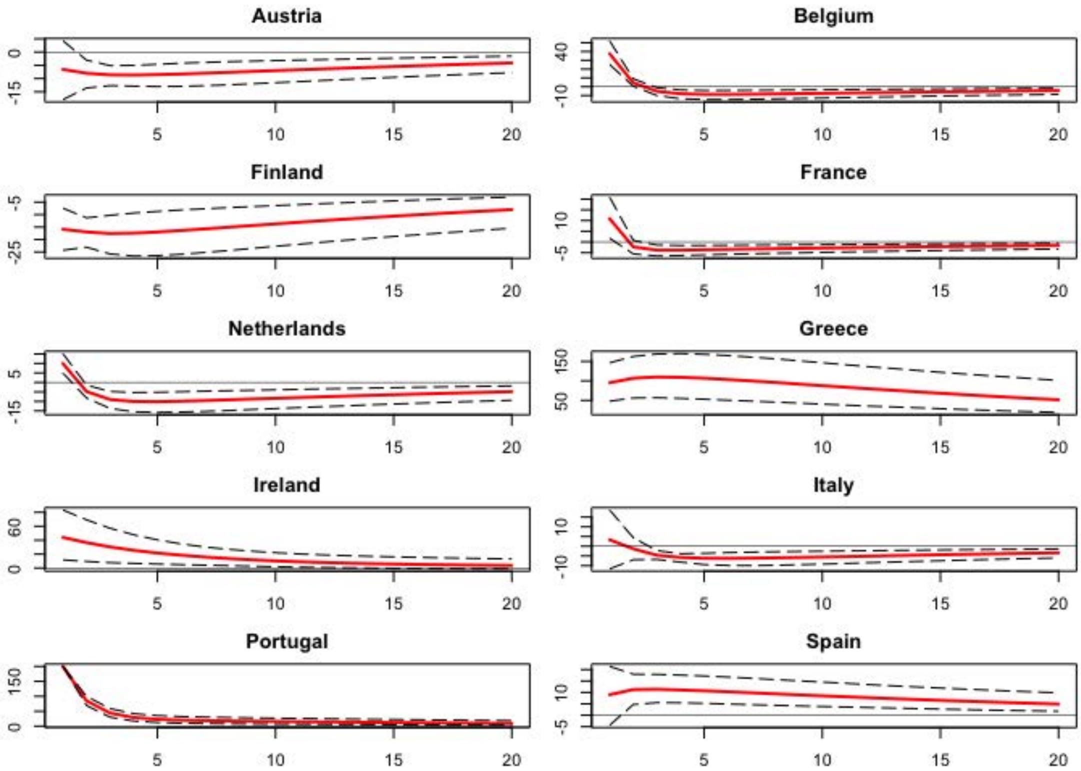

Figure D.16: The figure reports the Generalized Impulse Response Functions to a 200 b.p. shock to the 10Y Portuguese Spread in the pre-crisis period. [16^{th}, 84^{th}] confidence intervals are calculated using 10,000 bootstrap replications as in Appendix C.

Post-*ESD* crisis

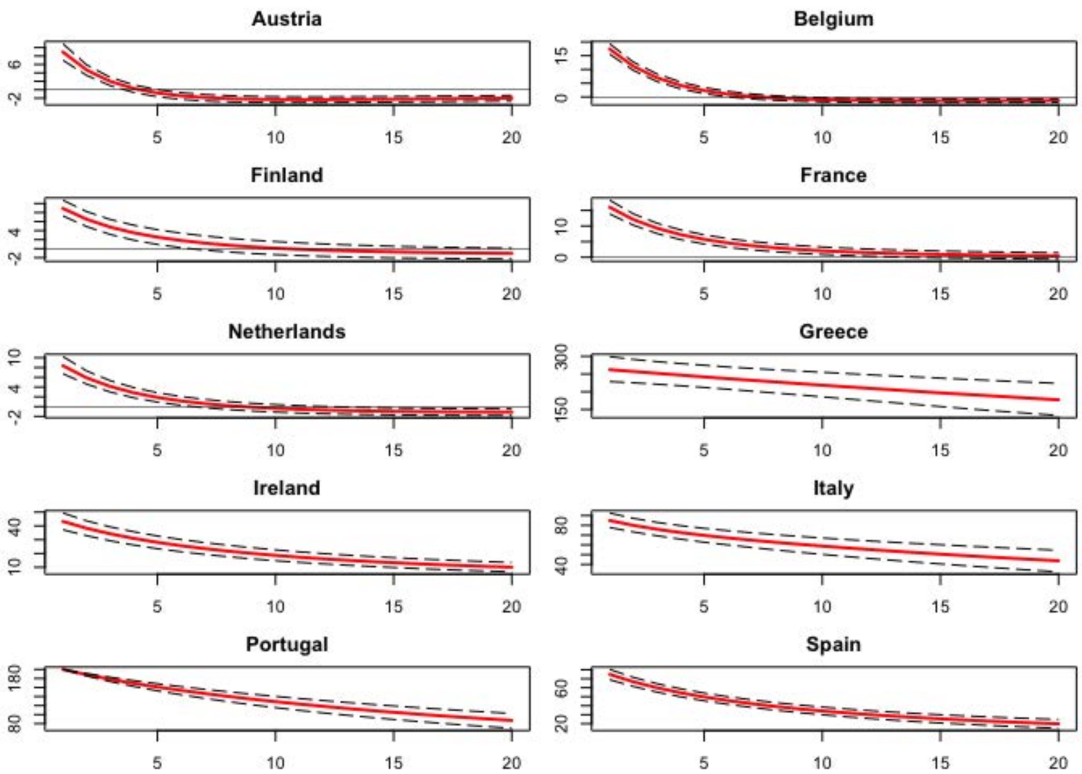

Figure D.17: The figure reports the Generalized Impulse Response Functions to a 200 b.p. shock to the 10Y Portuguese Spread in the post-crisis period. [16^{th}, 84^{th}] confidence intervals are calculated using $10,000$ bootstrap replications as in Appendix C.

COVID pandemic

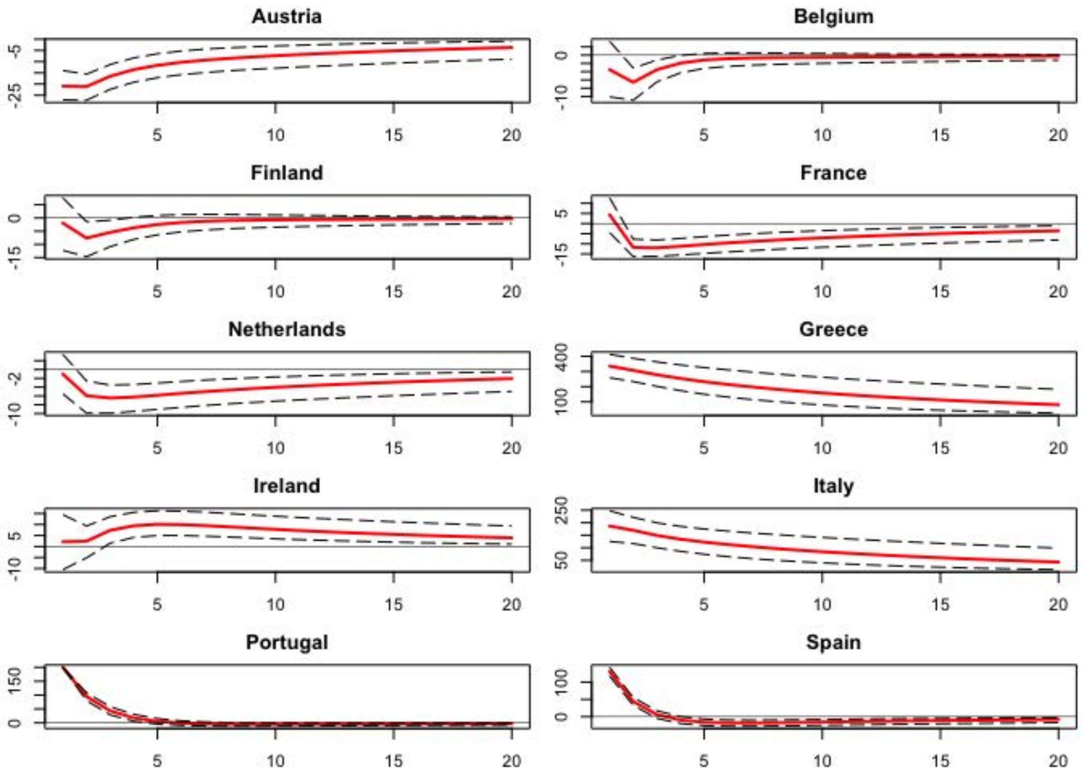

Figure D.18: The figure reports the Generalized Impulse Response Functions to a 200 b.p. shock to the 10Y Portuguese Spread in the COVID pandemic period. $[16^{th}, 84^{th}]$ confidence intervals are calculated using $10,000$ bootstrap replications as in Appendix C.